OPEN ACCESS Freely available online

PLoS GENETICS

The SUMO Isopeptidase Ulp2p Is Required to Prevent Recombination-Induced Chromosome Segregation Lethality following DNA Replication Stress

Ming-Ta Lee, Abla A. Bakir, Kristen N. Nguyen, Jeff Bachant*

Department of Cell Biology and Neuroscience, University of California Riverside, Riverside, California, United States of America

Abstract

SUMO conjugation is a key regulator of the cellular response to DNA replication stress, acting in part to control recombination at stalled DNA replication forks. Here we examine recombination-related phenotypes in yeast mutants defective for the SUMO de-conjugating/chain-editing enzyme Ulp2p. We find that spontaneous recombination is elevated in *ulp2* strains and that recombination DNA repair is essential for *ulp2* survival. In contrast to other SUMO pathway mutants, however, the frequency of spontaneous chromosome rearrangements is markedly reduced in *ulp2* strains, and some types of rearrangements arising through recombination can apparently not be tolerated. In investigating the basis for this, we find DNA repair foci do not disassemble in *ulp2* cells during recovery from the replication fork-blocking drug methyl methanesulfonate (MMS), corresponding with an accumulation of X-shaped recombination intermediates. *ulp2* cells satisfy the DNA damage checkpoint during MMS recovery and commit to chromosome segregation with similar kinetics to wild-type cells. However, sister chromatids fail to disjoin, resulting in abortive chromosome segregation and cell lethality. This chromosome segregation defect can be rescued by overproducing the anti-recombinase Srs2p, indicating that recombination plays an underlying causal role in blocking chromatid separation. Overall, our results are consistent with a role for Ulp2p in preventing the formation of DNA lesions that must be repaired through recombination. At the same time, Ulp2p is also required to either suppress or resolve recombination-induced attachments between sister chromatids. These opposing defects may synergize to greatly increase the toxicity of DNA replication stress.

Citation: Lee M-T, Bakir AA, Nguyen KN, Bachant J (2011) The SUMO Isopeptidase Ulp2p Is Required to Prevent Recombination-Induced Chromosome Segregation Lethality following DNA Replication Stress. PLoS Genet 7(3): e1001355. doi:10.1371/journal.pgen.1001355

Editor: Orna Cohen-Fix, National Institute of Diabetes and Digestive and Kidney Diseases, United States of America

Received September 22, 2010; **Accepted** February 25, 2011; **Published** March 31, 2011

Funding: This study was funded by NIH grant GM-661190 to JB. The funder had no role in study design, data collection and analysis, decision to publish, or preparation of the manuscript.

Competing Interests: The authors have declared that no competing interests exist.

* E-mail: jeffbach@citrus.ucr.edu

Introduction

As part of the DNA damage response, homologous recombination (HR), particularly template switch recombination through the post-replication DNA repair pathway (PRR), provides an important mechanism for restarting stalled replication forks and filling in un-replicated gaps in DNA (reviewed in [1,2]). These recombination events must be managed carefully, however. DNA strand exchange during HR, followed by re-initiating replication using the nascent sister chromatid as a template, can result in the formation of DNA linkages between daughter chromosomes. Failure to resolve these linkages, called sister chromatid junctions (SCJs), leads to chromosome breakage or aneuploidy, and may contribute to genome instability in many forms of cancer (reviewed in [3]).

A variety of studies implicate SUMO post-translational modification as an important regulator of HR in response to replication stress. Following activation of the SUMO precursor protein, SUMO modification is catalyzed by the E2 conjugating enzyme Ubc9p, which typically acts through one of several E3 ligases to covalently join SUMO moieties to lysine residues on substrate proteins (reviewed in [4]). One SUMO substrate that plays an especially prominent role in controlling HR at replication forks is Pol30p/PCNA, which is modified to recruit different activities to the replisome. During S phase, Ubc9p works through the E3 ligase Siz1p to sumoylate PCNA on K164 and K127 [5]. SUMO modified PCNA recruits the Srs2p helicase [6,7], which suppresses unscheduled HR by disassembling Rad51p nucleoprotein filaments [8-10]. Following replication fork stalling at MMS-induced DNA lesions, however, PRR proteins catalyze either mono- or poly-ubiquitinylation of PCNA K164 [5]. These modifications recruit trans-lesion bypass polymerases or induce template switching HR, respectively, providing alternative mechanisms to bypass the lesion and restart replication [5,11-13]. The existence of additional SUMO substrates that control HR is suggested by the observations that mutations affecting both Ubc9p and the E3 ligase Mms21p, which is not required for PCNA sumoylation, confer sensitivity to the replication impeding drugs hydroxyurea (HU) and methyl methansulfonate (MMS) [5,14-19]. Mms21p exists in a complex with two members of the structural maintenance of chromosomes family of proteins, Smc5p and Smc6p, which are also required for HU and MMS-resistance [15,16,20-22]. Notably, in response to MMS, *ubc9*, *mms21*, *smc5* and *smc6* mutants show an accumulation of X-shaped DNA structures that are thought to represent either regressed forks-a possible intermediate in fork restart-or hemi-catenate SCJs [17,19,23]. In this sense, they resemble mutants defective for the Sgs1p/Top3p/Rmi1p complex, which, through concerted heli-

Author Summary

DNA damage, arising from environmental stress or errors in DNA metabolism, can interfere with DNA replication. Cells respond by using homologous recombination to bypass the damage, resulting in DNA strand linkages between the replicated chromosomes. It is crucial to undo these linkages so chromosomes can segregate properly. Previously, a regulatory mechanism known as SUMO modification was shown to be important in controlling recombination following replication interference by the DNA damaging agent MMS. We show that mutations in a yeast enzyme called Ulp2p, which reverses SUMO modification, increase recombination and impose a requirement for recombination to maintain survival. MMS–treated *ulp2* mutants also accumulate recombination intermediates and fail to separate their chromosomes, leading to a permanent block to cell division. Further analysis suggests this block may not simply be due to a failure to resolve recombination intermediates, but may reflect a role for Ulp2p in undoing additional chromosome attachments that accompany recombination. In sum, our data indicate that cells defective for Ulp2p develop a love/hate relationship with recombination, requiring recombination for viability while failing to resolve chromosome attachments induced by recombination repair. Identification of Ulp2p substrates that ensure chromosome separation following recombination will shed light on how SUMO modification maintains genome stability.

case/topoisomerase activities, catalyzes the dissolution of hemicatenates and other DNA linkages [24-27]. These findings suggest complex roles for sumoylation in either preventing excessive/improper HR at stalled replication forks and/or mediating the active dissolution of SCJs.

As with the forward SUMO pathway, SUMO de-conjugation is also required to tolerate replication stress. Budding yeast contains two members of the SENP/Ulp family of SUMO isopeptidases, Ulp1p and Ulp2p, which catalyze removal of SUMO [28-30]. Ulp1p is an essential enzyme that is preferentially localized to the nuclear pore [28-32], whereas Ulp2p is distributed throughout the nucleus [29,30,33]. Ulp2p (first identified as Smt4p; [34]) is not essential, but *ulp2* mutants grow poorly and exhibit a complex assortment of phenotypes, including chromosome segregation and cell division defects. [29,30,35-42]. Ulp1p and Ulp2p also mediate functions that promote SUMO modification. Ulp1p is required to cleave the SUMO precursor to expose a glycine residue necessary for conjugation [28], while Ulp2p possesses a chain editing activity that prevents formation of aberrantly poly-sumoylated substrates [43]. Poly-sumoylation has the potential to interfere with the functional role of SUMO addition. Moreover, recent evidence has revealed that some poly-sumoylated substrates are targeted for degradation by the SUMO-targeted Slx5p-Slx8p ubiquitin ligase [44-46].

Although Ulp1p and Ulp2p play different roles in the SUMO pathway, one trait shared by *ulp1* and *ulp2* strains is that both exhibit sensitivity to HU and MMS [29,30,43]. Previously, a *ulp1-I615N* mutant was shown to accumulate single-stranded gaps during DNA replication, to exhibit increased spontaneous recombination, and to become dependent on Srs2p and HR for viability, suggesting a role for Ulp1p in suppressing replication errors that induce HR [47]. Insight into the replication stress sensitivity of *ulp2* mutants has come from the important finding that Ulp2p is required for cells to complete mitosis following DNA damage checkpoint arrest [41]. From this, de-sumoylation of Ulp2p substrates may be necessary to restart the chromosome segregation machinery once the checkpoint block to mitosis has been relieved [41,48]. But whether Ulp2p, like other components of the SUMO pathway, is also involved in controlling HR during DNA damage or replication stress has not yet been examined. In this study, we find that, following replication fork stalling by MMS, *ulp2* mutants accumulate persistent recombination intermediates that are likely to correspond to SCJs. This mis-regulation is accompanied by a severe, recombination-dependent, block to chromosome segregation, revealing a critical role for Ulp2p in allowing sister chromatids to disjoin following HR DNA repair.

Results

Recombination is elevated and essential in *ulp2* mutants

We initially set out to determine if *ulp2* mutants displayed a similar dependency on recombination as *ulp1-I615N* strains [47]. A *ulp2* deletion mutant (*ulp2*Δ) was mated to *rad52*Δ, *rad51*Δ and *rad6*Δ strains. Rad51p and Rad52p are required for most forms of HR [2], while Rad6p controls trans-lesion synthesis and template switching PRR [1]. *ulp2*Δ *rad52*Δ, *ulp2*Δ *rad51*Δ and *ulp2*Δ *rad6*Δ double mutants were either not obtained or were obtained at lower than expected frequencies from these crosses (Table 1, Table 2, Table 3). For *rad52*Δ, we examined this apparent synthetic lethality further by isolating *ulp2*Δ *rad52*Δ segregants harboring a wild type (WT) copy of *RAD52* on a *URA3* minichromosome (p*RAD52*). *ulp2*Δ *rad52*Δ/p*RAD52* mutants grew weakly, if at all, on media containing 5-FOA, a drug that only allows growth if cells are capable of losing p*RAD52* (Figure 1A). Thus, Rad52p is essential for proliferation of *ulp2*Δ cells.

The essential role of Rad52p prompted us to examine whether HR was elevated in the absence of Ulp2p. Yeast cells exhibit a uniform nuclear distribution of fluorescent Rad52p-GFP in the absence of DNA damage (Figure 1B, [49]), but Rad52p-GFP rapidly assembles into intra-nuclear foci during HR DNA repair [49]. We found that an average of 17% of *ulp2*Δ cells in mid-logarithmic phase cultures displayed Rad52p-GFP foci, a significant increase ($p = 0.0074$) compared to less than 1% in WT cells. (Figure 1B). As a second assay, we utilized a reporter in which recombination events between direct repeats on chromosome XV can be selected because they restore an intact *HIS3* gene [50]. *ulp2*Δ cells exhibited a 4.7-fold increase in the median frequency of this form of recombination (Figure 1C; $p = 0.044$), indicating spontaneous HR at this genomic locus is significantly increased in *ulp2*Δ mutants.

Ulp2 mutants display a reduced frequency of chromosome rearrangements

DNA replication errors are potent inducers of HR and can initiate chromosome rearrangements [51,52]. Based on this, we used a yeast artificial chromosome (YAC) assay to examine the frequency of spontaneous gross chromosomal rearrangements (GCRs) in *ulp2*Δ cells ([53]; Figure 2A). For comparison, we also measured GCR frequencies in *ulp1-333*, *smt3-331* and *ubc9-1* SUMO pathway mutants (*SMT3* encodes the single SUMO isoform in budding yeast). Using the YAC system, we obtained median GCR frequencies of 252×10^{-7} for WT cells, 5490×10^{-7} for *smt3-331* cells, 6109×10^{-7} for *ubc9-1* cells, and 2617×10^{-7} for *ulp1-333* cells (Figure 2B), representing 22-, 24-, and 10-fold increases, respectively, compared to WT controls. In contrast, and counter to initial expectations, it proved difficult to recover spontaneous GCRs in *ulp2*Δ mutants, with a median GCR frequency of 56×10^{-7} (Figure 2C). This represents a significant ($p = 0.025$) 4.5-fold decrease compared to WT.

Table 1. Genetic interactions between *ulp2*Δ and *rad52*Δ mutants.

Cross between JBY238 and JBY270; *ulp2*Δ × *rad52*Δ; 26 tetrads		
Genotype	**# Expected Spores**	**# Obtained (% of Expected)**
WT	26	18 (69%)
*ulp2*Δ	26	18 (69%)
*rad52*Δ	26	32 (123%)
*ulp2*Δ *rad52*Δ	26	2 (8%)
Total	104	70 (67%)

doi:10.1371/journal.pgen.1001355.t001

To further monitor chromosome rearrangements we examined two circular dicentric minichromosomes. In one (p2X*CEN*$^{\text{direct}}$), two copies of a *CEN* sequence were oriented in a direct repeat configuration. In the other (p2X*CEN*$^{\text{invert}}$), the same *CEN* duplication was oriented as inverted repeats. Previous studies have shown that both direct and inverted repeat dicentrics can be efficiently transformed into yeast, and are initially retained through a combination of co-orientation of the two *CEN*s on the spindle and non-disjunction following dicentric bridging [54,55]. During outgrowth, however, rearranged minichromosomes that have deleted one of the *CEN*s accumulate. For direct *CEN* repeats these deletions tend to arise through loop out events, whereas inverted *CEN* repeats are resolved through more complex re-arrangements. Consistent with this characterization, in WT transformants p2X*CEN*$^{\text{direct}}$ and p2X*CEN*$^{\text{invert}}$ exhibited similar mitotic stabilities to p1X*CEN* controls (Figure 2D). Analysis of minichromosomes rescued from these cells revealed precise *CEN1* excision for p2X*CEN*$^{\text{direct}}$ and a diversity of plasmid species for p2X*CEN*$^{\text{invert}}$ (not shown). In *ulp2*Δ mutants, p1X*CEN* was only retained in ~30% of the cells; this result is in keeping with previous studies showing reduced minichromosome stability in the absence of Ulp2p [29]. p2X*CEN*$^{\text{direct}}$ demonstrated a similar stability to p1X*CEN* (Figure 2D), and underwent the same precise *CEN* deletions observed in WT (not shown). In contrast, p2X*CEN*$^{\text{invert}}$ proved extremely unstable, with less than 1% of *ulp2*Δ cells maintaining the mini-chromosome. These results suggest that some chromosome re-arrangements either fail to occur or cannot be tolerated in *ulp2* mutants.

Table 2. Genetic interactions between *ulp2*Δ and *rad51*Δ mutants.

Cross between JBY238 and JBY310; *ulp2*Δ × *rad51*Δ; 26 tetrads		
Genotype	**# Expected Spores**	**# Obtained (% of Expected)**
WT	26	16 (69%)
*ulp2*Δ	26	22 (85%)
*rad51*Δ	26	24 (92%)
*ulp2*Δ *rad51*Δ	26	6 (23%)
Total	104	68 (65%)

doi:10.1371/journal.pgen.1001355.t002

Table 3. Genetic interactions between *ulp2*Δ and *rad6*Δ mutants.

Cross between JBY238 and JBY285; *ulp2*Δ × *rad6*Δ; 22 tetrads		
Genotype	**# Expected Spores**	**# Obtained (% of Expected)**
WT	22	18 (82%)
*ulp2*Δ	22	10 (45%)
*rad6*Δ	22	18 (82%)
*ulp2*Δ *rad6*Δ	22	0 (0%)
Total	88	46 (52%)

doi:10.1371/journal.pgen.1001355.t003

MMS–induced HR intermediates accumulate in *ulp2*Δ mutants

In order to more directly examine the consequences of HR in *ulp2*Δ mutants, we used MMS to induce recombination. As an initial experiment, we examined chromosome integrity following exposure to MMS by pulse-field gel electrophoresis. WT and *ulp2*Δ cells were arrested in G1, released into media containing 0.01% MMS for 2 hr, and then allowed to recover in MMS-free media. Following MMS treatment a lower molecular weight DNA smear was observed in both WT and *ulp2*Δ strains (Figure 3A), reflecting MMS-induced chromosome breakage [17]. For both strains, a one hr recovery largely restored the normal chromosome banding pattern. This suggests Ulp2p is not obviously required for healing MMS-induced DNA breaks.

We next examined processing of MMS-induced DNA lesions. In the experiment shown in Figure 3B, WT cells and *ulp2*Δ mutants expressing *RAD52-GFP* were treated with 0.01% MMS and allowed to recover. After a 2 hr recovery, ~30% of WT cells accumulated Rad52p-GFP foci (Figure 3B). By 6 hr, however, the percentage of cells with Rad52p-GPF foci had substantially declined and many cells were proceeding with the next round of cell division. In contrast, *ulp2*Δ mutants showed a much stronger accumulation of Rad52p-GFP foci, reaching a maximum of ~60% (Figure 3B), and these foci tended to persist for the duration of the recovery period. We also examined Rad52p-GFP foci in *ulp2*Δ cells treated with 200 mM HU. HU does not normally induce Rad52p foci because the integrity of the replisome is maintained by the S phase checkpoint (Figure 3B, [56]). HU treated *ulp2*Δ cells, however, exhibited a strong induction of Rad52p-GFP foci.

In response to MMS, proper regulation of HR is required to prevent X-shaped recombination intermediates from accumulating in the vicinity of origins of replication [17,19,23]. On two-dimensional gels these structures migrate as a "X-spike" that is distinct from replication forks and bubbles [57,58]. To determine whether *ulp2*Δ mutants accumulated this type of HR intermediate, *ulp2*Δ cells, along with WT and *sgs1*Δ controls, were released from a G2/M nocodazole block and treated with 0.033% MMS for 3 hr as previously described [17]. Genomic DNAs were fractionated on two-dimensional gels, and probed with a DNA fragment corresponding to ARS305. A prominent X-spike signal was observed in *sgs1*Δ and *ulp2*Δ samples (Figure 3D). Thus, Ulp2p deconjugating and/or chain editing activities are required to prevent accumulation of MMS-induced HR intermediates.

Interactions between Ulp2p and Sgs1p

Based on current evidence, Sgs1p is one SUMO target that could be connected to Ulp2p's role in HR. In particular, a recent

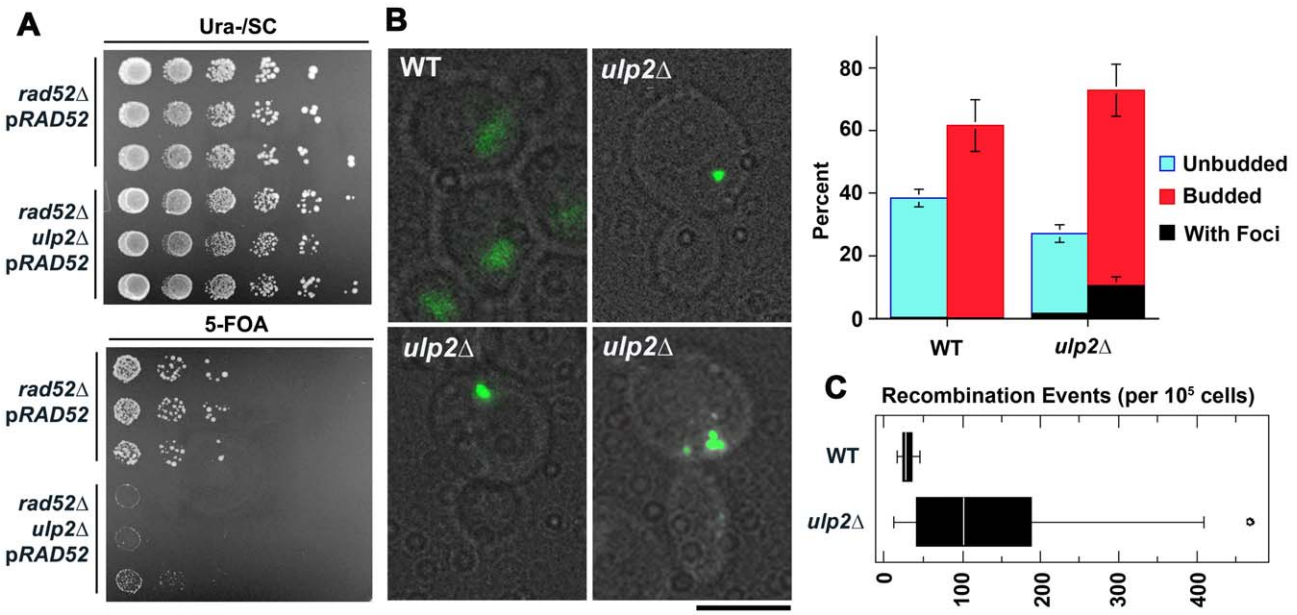

Figure 1. Spontaneous HR in *ulp2*Δ mutants. (A) *rad52*Δ and *ulp*Δ *rad52*Δ segregants harboring p*RAD52-URA3* were derived from a cross between *rad52*Δ/p*RAD52-URA3* (MLY031; p*RAD52* is pVL191) and *ulp2*Δ (JBY238) haploid strains, cultured in the absence of selection for p*RAD52-URA3*, and a 10-fold dilution series was stamped onto Ura$^-$/SC (growth requires p*RAD52-URA3*) and 5-FOA media (growth requires loss of p*RAD52-URA3*). Plates were cultured at 30°C and photographed after 3 days. (B) Aliquots of mid-log phase cultures of WT (MLY061) and *ulp2*Δ (MLY060) *RAD52-GFP* strains were fixed and scored to determine the percentage of unbudded and budded cells exhibiting distinct Rad52p-GFP foci. Micrographs (superimposed bright field and fluorescent images) depict dispersed nuclear Rad52p-GFP signal in WT cells and Rad52p-GFP foci in *ulp2*Δ mutants. Scale bar, 4 μm. Graph displays the average percentage of budded and un-budded cells with and without Rad52p foci determined from three separate experiments. Error bars, ± one standard deviation. A total of 1,018 WT and 523 *ulp2*Δ cells were scored; 4 WT cells displayed distinct foci (0.4%). The p value (Student's t-test) for comparing total number of cells with foci from the WT and *ulp2*Δ datasets is 0.0074. (C) WT (MLY066; 8 cultures) and *ulp2*Δ (MLY067; 10 cultures) strains were constructed in which a plasmid insertion at the *HIS3* locus is flanked by 414 bp direct repeats. Recombination events between the repeats can be selected because they restore *HIS3* function. Box plot graphs display the median number of His$^+$ clones per 10^5 viable cells, 25th and 75th percentiles, and range of data (p = 0.044; Student's t-test).
doi:10.1371/journal.pgen.1001355.g001

study has shown that a single prominent SUMO species of Sgs1p accumulates after MMS exposure, and K621 has been identified as the acceptor lysine that is responsible for this modification [59]. We were able to confirm that treatment with 0.3% MMS resulted in a substantial fraction of Sgs1p-myc shifting into a reduced mobility species (Figure 4A and Figure S1), and that a decreased amount of this form was observed following treatment with a lower MMS concentration (0.033%; Figure 4B, 4C). The appearance of this form was abolished in *ubc9-1* strains (Figure 4B) and a *sgs1-K621R* mutant (Figure S1), indicating it is likely to correspond to the previously reported K621 conjugate. In *ulp2*Δ strains, however, a marked increase in this putative Sgs1p SUMO species was observed (Figure 4B, 4C), which persisted for at least 3 hr after removal of MMS (Figure 4C). In sum, these results suggest that sumoylation of Sgs1p is likely to be regulated by Ulp2p.

If failure to properly control Sgs1p sumoylation was responsible for *ulp2*Δ HR defects, SUMO-resistant Sgs1p might ameliorate these phenotypes. We therefore examined whether a plasmid-born copy of the *sgs1-K621R* allele could prevent Rad52p foci accumulation. Following a two hr treatment with 0.010% MMS, however, no significant reduction in *ulp2*Δ *sgs1-K621R* cells displaying Rad52p-GFP foci was observed (Figure 4D). Previous studies have shown that a form of Smt3 (*smt3-3KR*) that cannot form polymeric SUMO chains can rescue the HU and MMS sensitivity of *ulp2* mutants [43], leading us to test whether *smt3-3KR* could prevent Rad52p foci accumulation. This proved to be the case, as *smt3-3KR ulp2*Δ double mutants did in fact show a substantial reduction in the accumulation of both spontaneous and MMS-induced Rad52p foci (Figure 4F). Thus, proper SUMO chain editing through Ulp2p is likely to be important in controlling HR.

*ulp2*Δ mutants fail in chromosome segregation after exposure to MMS

In our experiments, it was apparent that *ulp2*Δ cells frequently remained blocked in the cell cycle during recovery from MMS, similar to previous results examining *ulp2* recovery following HU treatment and in response to an irreparable DNA double strand break [41]. We took four experimental approaches to investigate the basis for the apparent MMS recovery defect of *ulp2*Δ cells. First, phospho-activation of the Rad53p checkpoint kinase during the DNA damage response results in a series of slower migrating gel mobility variants [60], and collapse of these forms provides a means to assess silencing of the checkpoint. In WT cells, Rad53p phospho-variants almost completely disappeared during a 2–4 hr recovery after treatment with 0.01% MMS (Figure 5A). A similar pattern was observed in *ulp2*Δ strains, although the accumulation and disappearance of shifted Rad53p appeared to be slightly delayed.

Second, we examined degradation of Pds1p/securin. Pds1p is a downstream target of the DNA damage checkpoint that is stabilized to block cohesin proteolysis and anaphase entry [61,62]. The kinetics of Pds1p degradation therefore provides a read-out of commitment to anaphase. In these experiments, we used the *cdc14-1* allele to block Pds1p re-synthesis once cells recovered from the checkpoint. *cdc14-1 PDS1-myc* and *cdc14-1 ulp2*Δ *PDS1-myc* cells were treated with 0.001%, 0.005% and 0.01% MMS for 2 hr, allowed to recover at a *cdc14-1* non-

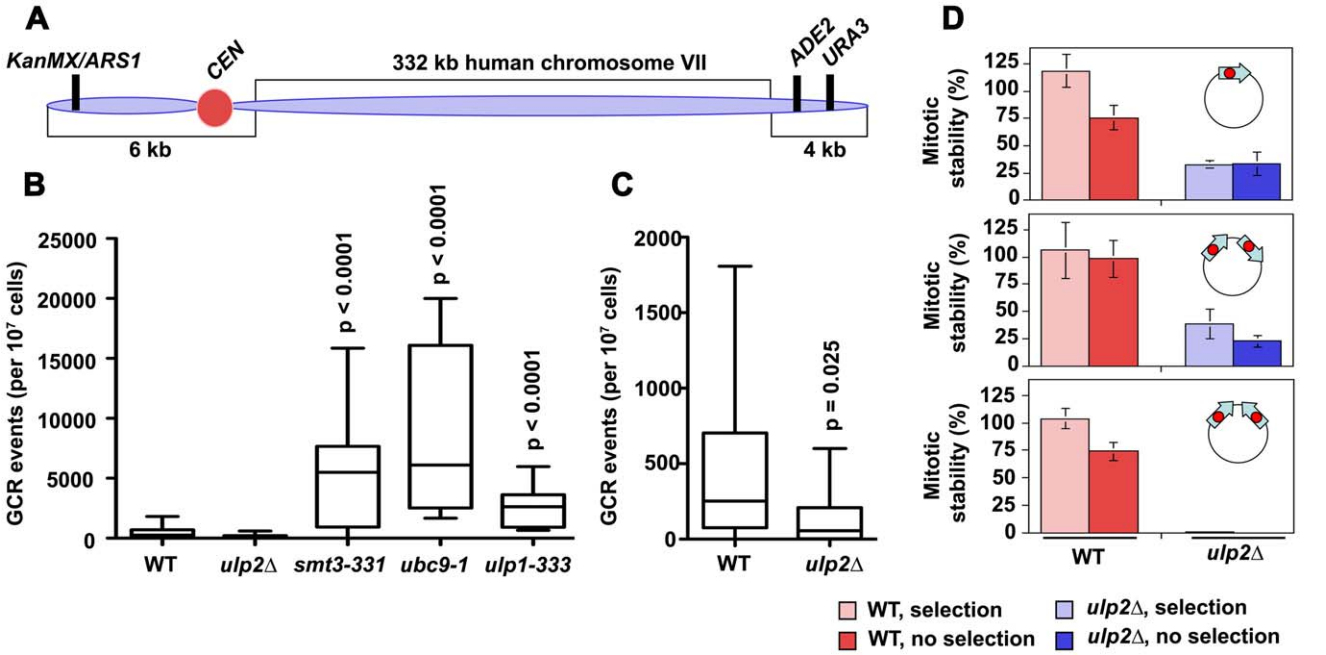

Figure 2. Chromosome re-arrangements in *ulp2*Δ mutants. (A) The YAC used for GCR analysis consists of an origin of replication (*ARS1*), a *CEN*, and a long right arm containing 332 kbp of human DNA (adapted from [53]). GCRs deleting *ADE2/URA3* at the terminus of right arm can be selected and distinguished from YAC loss through segregation errors. (B) WT (MLY068; 30 cultures), *ulp2*Δ (MLY069; 30 cultures), *smt3-331* (MLY070; 10 cultures), *ulp1-333 (*MLY071; 10 cultures) and *ubc9-1* (MLY072; 10 cultures) strains harboring the YAC were plated onto 5-FOA media to select for loss of *URA3* and further genotyped to identify GCRs. Box plot graphs display median GCR events per 10^7 viable cells. p values (Student's t-test) were obtained from pair-wise comparisons between indicated mutants and the WT control. (C) Data as in B, but with lowered y-axis scale to show the reduction of GCRs in the *ulp2*Δ strain. It is possible to calculate that an average of 97.8±1.7% of WT cells and 93.6±4.4% of *ulp2*Δ cells retained the YAC at the time of plating to select for GCRs. (D) WT (CRY1) and *ulp2*Δ (JBY242) strains were transformed with three circular *URA3* minichromosomes: monocentric p1X*CEN*, dicentric p2X*CEN*^{direct}, and dicentric p2X*CEN*^{invert}. Nine transformants for each strain/plasmid combination were cultured in parallel YPD (no selection for minichromosome) or Ura$^-$/SC (to maintain selection) media, and equivalent volumes were plated onto YPD and Ura$^-$/SC media. Graphs display the average percentage of cells retaining the minichromosome (mitotic stability), ± one standard deviation.
doi:10.1371/journal.pgen.1001355.g002

permissive temperature, and Pds1p-myc abundance was monitored over a 24 hr period. In *cdc14-1* cells, Pds1p-myc degradation proceeded in a dose-dependent manner until 10 hr post-treatment (Figure 5B, 5C). At this point, Pds1p started to increase in the 0.001% and 0.005% MMS cultures, probably reflecting leakage through the *cdc14-1* arrest. These degradation kinetics were virtually indistinguishable in *cdc14-1 ulp2*Δ cells, although re-synthesis of Pds1p was not observed (Figure 5B, 5C). These results suggest that MMS treated *ulp2*Δ cells can terminate checkpoint signaling and commit to anaphase.

Third, we used micro-colony analysis to determine whether getting rid of the checkpoint relieved the restraint on cell division. Cells from MMS treated and untreated cultures were positioned on agar plates, and the appearance of cell bodies was examined over time. A budded yeast cell arrested at the DNA damage checkpoint consists of two cell bodies. If this cell completes mitosis and one of progeny cells sends forth a bud, the microcolony now contains three cell bodies, and the number of cell bodies increases exponentially with continued division. We found that an average of 68% of WT cells were able to form microcolonies containing ≥ 16 cell bodies within a 3 day period after transient exposure to MMS, indicating the majority recovered efficiently (Figure 6). In comparison, even in the absence of MMS, 20% of *ulp2*Δ cells remained blocked at the 2–3 cell body stage. This lethality was strongly exacerbated by MMS treatment, with 64% of *ulp2*Δ cells failing to proliferate beyond 2–3 cell bodies. Inactivating the DNA damage checkpoint in *rad9*Δ *ulp2*Δ mutants, or both the DNA damage and S phase checkpoints in *mec1*Δ *ulp2*Δ mutants, did not relieve the *ulp2*Δ block to cell division (Figure 6). *ulp2* cells fail to maintain chromatid cohesion at centromeric regions during DNA damage checkpoint arrest [36,42], which could potentially activate the spindle assembly checkpoint (SAC). We therefore tested whether abolishing the SAC could restore *ulp2*Δ division. However, ~60% of MMS treated *ulp2*Δ *mad2*Δ mutants still remained blocked with 2–3 cell bodies (Figure S2). We further generated a *ulp2*Δ *rad9*Δ *mad2*Δ triple mutant to abolish both DNA damage and SAC checkpoint responses. This triple mutant grew extremely poorly, and, following exposure to MMS, ~90% of the cells failed to recover (Figure 6). Thus, MMS treated *ulp2*Δ mutants experience a terminal block to cell division even in the absence of pre-anaphase checkpoint controls.

Fourth, we examined mitotic progression in *ulp2*Δ cells by cytology and flow cytometry. Following a 2 hr treatment with 0.01% MMS, WT cells arrested at the DNA damage checkpoint typically showed short pre-anaphase spindles and an undivided mass of chromatin (Figure 7A, 7B). Completion of mitosis during recovery was characterized by normal spindle extension and chromosome transmission. As monitored by DAPI staining and a Lac operator-GFP chromosome tag (*TRP1-GFP*), ~70% of *cdc14-1* cells underwent chromosome separation and segregation during recovery (Figure 8A, 8B), and FACS analysis indicated that many cells proceeded with additional rounds of cell division (Figure S3). In contrast, many MMS treated *ulp2*Δ cells showed partial, incomplete spindle extension during recovery, accompanied by an apparent block to nuclear division (Figure 7A, 7B). In some cells it was possible to visualize chromatin fibers that appeared to be

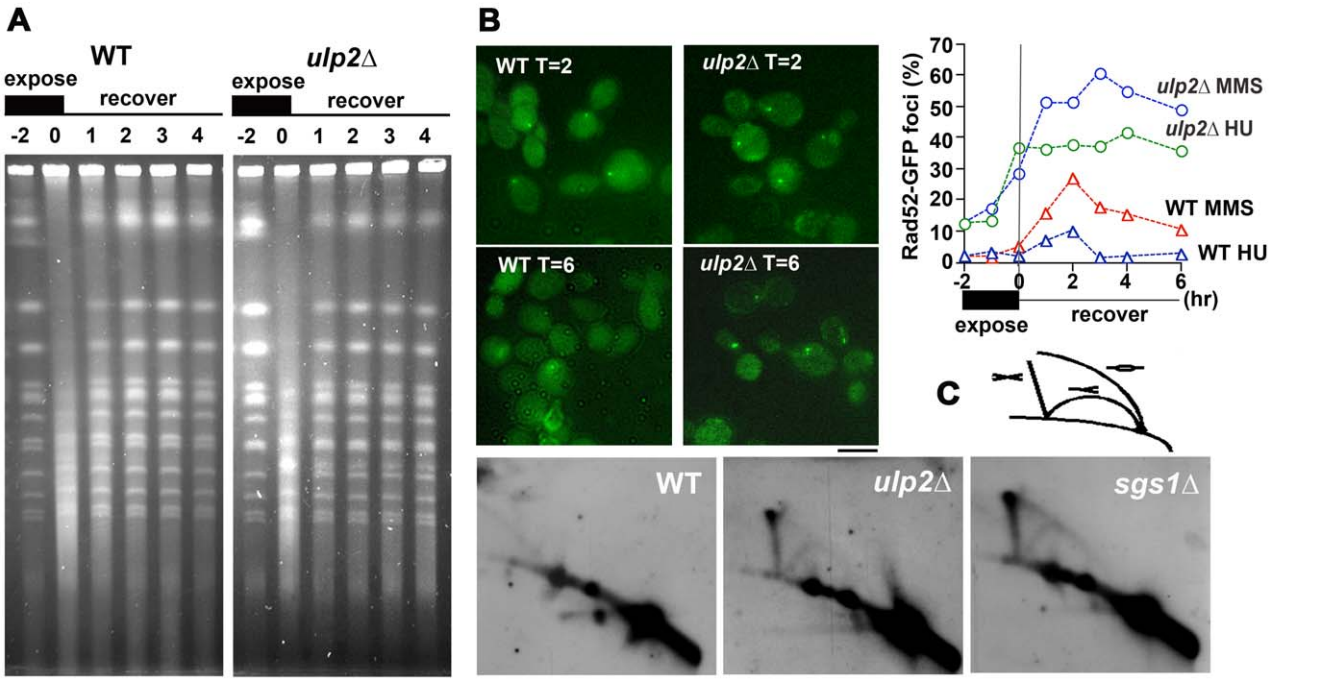

Figure 3. MMS–induced HR in *ulp2*Δ mutants. (A) Pulse field gel analysis of chromosome integrity. WT (JBY1129) and *ulp2*Δ mutant (JBY1309) cells were arrested in G1 with mating pheromone and released (−2 hr time point) into media containing 0.01% MMS. After 2 hr, cells were washed into MMS-free YPD pH 3.9 media and allowed to recover (recovery begins at the 0 hr time point). Mating pheromone was added to restore the G1 block once cells recovered from DNA damage checkpoint arrest and completed mitosis. At the indicated times, samples were prepared for pulse-field gel electrophoresis and DNA was visualized by ethidium bromide staining. (B) Analysis of Rad52p foci. Cultures of WT (MLY061) and *ulp2*Δ (MLY060) *RAD52-GFP* strains were treated with either 0.01% MMS or 200mM HU for 2 hrs (−2 hr to 0 hr time points) and allowed to recover in fresh media. Aliquots were fixed and scored for the appearance of distinct Rad52p foci; at least 100 cells were scored per time point. On graph, WT in HU and MMS (triangles); *ulp2*Δ in HU and MMS (circles). Micrographs display fluorescent images of MMS-treated cells following either a 2 hr or 6 hr recovery period. Scale bar, 4 µm. (C) Two-dimension gel analysis of HR intermediates. WT (MLY080), *ulp2*Δ (MLY085), and *sgs1*Δ (MLY082) cells were synchronized in G2/M using nocodazole and released into media containing 0.033% MMS. After 3 hr, genomic DNA samples were fractionated on two-dimensional gels, transferred to nitrocellulose, and hybridized to a DNA fragment encompassing ARS305 (an early-firing origin of replication) to detect HR or DNA replication structures. Schematic depicts the relative migration of replication bubbles, forks and X-spike HR intermediates.
doi:10.1371/journal.pgen.1001355.g003

pulled away from an undivided mass of chromatin (Figure 7B iii; arrows). In others, chromosome separation appeared more complete, but chromatin was stretched to varying degrees along the spindle (Figure 7B iv). DAPI staining indicated less than 20% of *cdc14-1 ulp2*Δ cells successfully completed chromosome segregation (Figure 8A). ~30% of *cdc14-1 ulp2*Δ cells underwent *TRP1-GFP* separation during recovery, but the separated foci largely failed to segregate (Figure 8B). FACS analysis suggested that MMS treated *ulp2*Δ cells potentially tried to proceed with a second round of DNA replication following this block chromosome segregation, although the FACS profiles were quite heterogeneous and did not clearly resolve into a peak of cells with a 4N content of DNA (Figure S3).

Since *sgs1*Δ and *ulp2*Δ mutants both accumulate HR intermediates that might be expected to link sister chromatids (Figure 3C), we additionally examined chromosome segregation during MMS recovery in *cdc14-1 sgs1*Δ cells. Compared to the *ulp2*Δ defect, the fraction of MMS treated *cdc14-1 sgs1*Δ cells that could segregate their chromosomes to an extent necessary to form two distinct nuclear masses was only slightly reduced compared to *cdc14-1* controls (Figure 8A; see Figure S4 for a more complete description). Taken as a whole, these results allow us to conclude that, although they commit to anaphase, *ulp2*Δ mutants are unable to separate their chromosomes efficiently following MMS treatment. Furthermore, this non-disjunction defect appears more severe than that observed in a *sgs1*Δ strain.

Blocking HR restores chromosome segregation in MMS–treated *ulp2* mutants

If defective HR in MMS treated *ulp2*Δ cells is causally linked to the chromosome separation defect that we observed in our experiments, blocking recombination should restore chromosome segregation. Given that HR is essential in *ulp2*Δ mutants (Figure 1) our approach to test this was to overproduce (OP) the Srs2p helicase. In addition to antagonizing nucleoprotein filament assembly [8-10], Srs2p also appears to exert anti-recobinogenic activity by unwinding D-loop intermediates [63,64]. Srs2p OP should therefore be an effective way to short circuit early stages of HR. *cdc14-1*, *cdc14-1 rad9*Δ, *cdc14-1 ulp2*Δ and *cdc14-1 rad9*Δ *ulp2*Δ strains were transformed with a vector control or a high copy plasmid in which *SRS2* was expressed under control of its endogenous promoter (p*SRS2*). The transformants were then treated with 0.01% MMS for 2 hr and allowed to recover at a *cdc14-1* non-permissive temperature. Compared to vector controls, *cdc14-1*/p*SRS2* cells remained blocked in a pre-anaphase configuration for the duration of the recovery period (Figure 9A). This delay was abolished in *cdc14-1 rad9*Δ/p*SRS2* transformants, suggesting Srs2p OP was able to prolong DNA damage checkpoint arrest. In the absence of Ulp2p, however, inactivating the checkpoint in the *cdc14-1 rad9*Δ *ulp2*Δ/vector strain was insufficient to allow cells to proceed with chromosome segregation (Figure 9A, 9B). Significantly, Srs2p OP demonstrated a remarkable ability to allow *ulp2*Δ strains to escape this mitotic

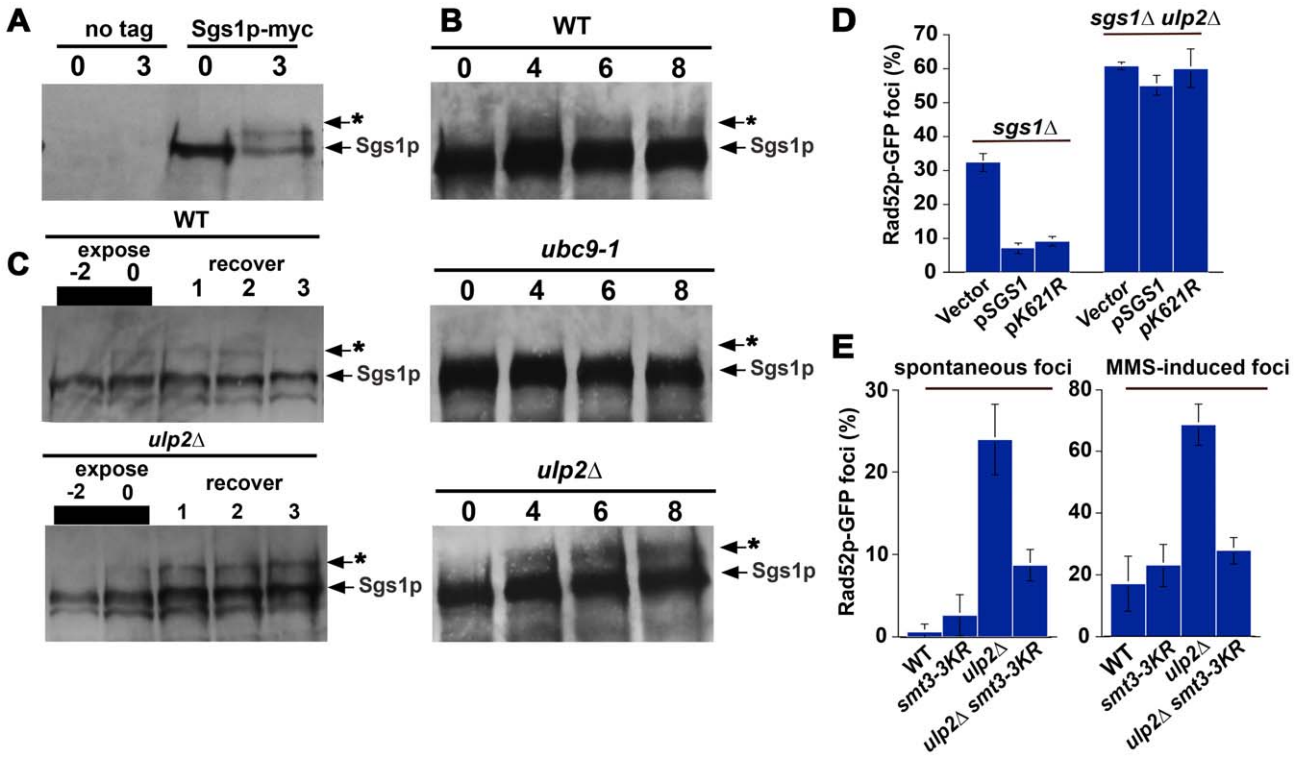

Figure 4. Sgs1p sumoylation in *ulp2*Δ mutants. (A) WT cells either lacking (CRY1; no tag) or expressing (MLY157; Sgs1p-myc) 18Xmyc-tagged *SGS1* were washed into YPD media containing 0.3% MMS (0 time point) and treated for 3 hr. Protein samples prepared at the 0 and 3 hr time points were analyzed by α-myc immunoblotting. (B) WT (MLY157), *ubc9-1* (MLY165) and *ulp2*Δ (MLY162) *SGS1-myc* strains cultured at 23°C were washed into 0.033% MMS media at 35°C and continuously treated for 8 hr. Protein samples were prepared at the indicated times and examined for Sgs1p-myc electrophoretic mobility by α-myc immunoblotting. (C) WT (MLY157) and *ulp2*Δ (MLY162) *SGS1-myc* strains were treated with 0.033% MMS for two hr (−2 to 0 time points), and allowed to recover in MMS-free media for an additional 3 hr. Protein samples were analyzed by α-myc immunoblotting. In (A, B and C), arrow with asterisk indicates the putative Sgs1p K621 SUMO conjugate [59]. (D) *sgs1*Δ (MLY200) and *sgs1*Δ *ulp2*Δ (MLY144) strains harboring *RAD52-GFP* were transformed with a vector control (pRS426;[84]), a plasmid expressing *SGS1* (p*SGS1*; YCplac33/*SGS1*;[85]) or a plasmid expressing a *sgs1-K621R* mutant allele (p*sgs1-K621R*; pJBN269). Three transformants for each strain/plasmid combination were treated with 0.01% MMS for 2 hr and allowed to recover in MMS-free media. After a 6 hr recovery, aliquots were fixed and scored to determine the percentage of cells with Rad52p-GFP foci. Graphs display the average of the three cultures, ± one standard deviation. (E) Aliquots of logarithmic phase cultures of three WT (MLY061, JBY1815, JBY1816), *smt3-3KR* (JBY1817-1819), *ulp2*Δ (JBY1820-1822), and *ulp2*Δ *smt3-KR* (JBY1823-1825) strains harboring *RAD52-GFP* were fixed and evaluated as in (D) to determine the percentage of cells displaying spontaneous Rad52-GFP foci (spontaneous foci graph). In parallel, the same set of cells was also treated with 0.01% MMS, allowed to recover for 6 hr, and scored for persistence of Rad52-GFP foci (MMS-induced foci graph).
doi:10.1371/journal.pgen.1001355.g004

block, with ~50% of *cdc14-1 rad9*Δ *ulp2*Δ/p*SRS2* cells now segregating their chromosomes in a seemingly normal anaphase (Figure 9A, 9B). Thus, Srs2p OP substantially relieves the block to chromosome separation in MMS treated *ulp2*Δ cells.

Discussion

HR and genome stability in *ulp2* mutants

One principal finding of this study is that, even in the absence of exogenous DNA replication stress, spontaneous recombination is increased in *ulp2*Δ cells. This conclusion is based on two observations. First, by genetic criteria, spontaneous recombination at a genomic location on chromosome XV is elevated in *ulp2*Δ strains. Second, *ulp2*Δ mutants also display an increase in the frequency of spontaneous Rad52p DNA repair foci. A similar increase in Rad52p foci has been observed in a number of other SUMO pathway mutants, and has been shown to be largely attributable to a requirement for sumoylation in preventing inappropriate recombination events involving the 2 μm circle, an endogenous plasmid found in most *S. cerevisiae* strains [65]. Since we have not directly examined the effect of the 2 μm circle on recombination in *ulp2* mutants, destabilization of this extrachromosomal element may well contribute to the *ulp2*Δ increase in Rad52p foci. However, as the 2 μm circle is not required for *S. cerevisiae* growth, our finding that HR DNA repair becomes essential in *ulp2*Δ strains strongly suggests that Ulp2p acts to suppress the formation of genomic DNA lesions that must be repaired through recombination. Previous analyses of the SUMO pathway support this possibility. For example, SUMO conjugation-defective *ubc9-1* mutants exhibit synthetic growth defects in the absence of HR and, at the non-permissive temperature, accumulate DNA structures that activate Rad53p [17]. Furthermore, as described in the Introduction, *ulp1-I615N* mutants also show increased HR and require HR for viability; in this case, the requirement for HR was shown to correspond with single-stranded DNA gaps arising during S phase [47]. It is striking that perturbations to Ulp1p and Ulp2p, which appear to target largely distinct sets of SUMO substrates [29], impose such seemingly similar dependencies on HR. Another observation that lends credence to the idea that Ulp2p suppresses recombinogenic DNA lesions is that *ulp2*Δ mutants greatly induce the formation of Rad52p foci following HU treatment. Such foci are not observed

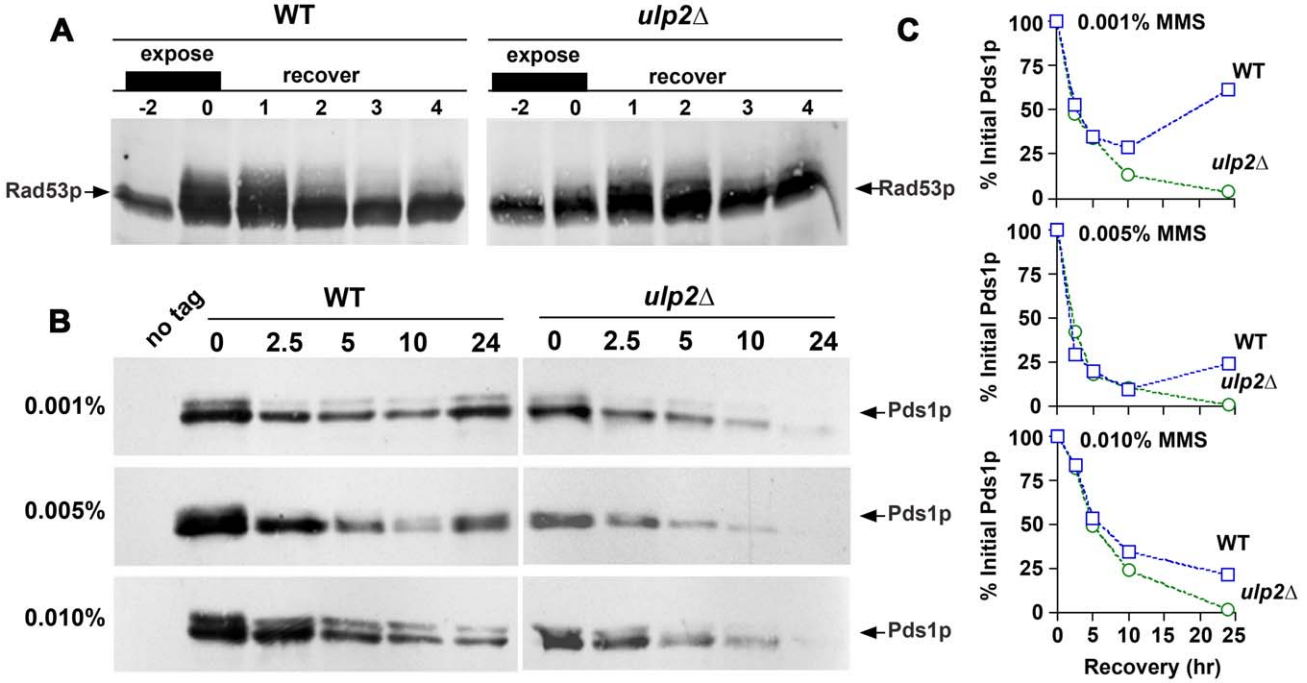

Figure 5. *ulp2*Δ mutants terminate checkpoint signaling and commit to anaphase after MMS treatment. (A) Rad53p activation/de-activation. WT (CRY1) and *ulp2*Δ (JBY240) mutants were synchronized in G1 using mating pheromone, then released into media containing 0.01% MMS (−2 hr time point). After a 2 hr MMS treatment (0 hr time point) cells were allowed to recover in MMS-free media, and mating pheromone was restored to re-arrest cells in the next G1. Protein samples were analyzed by α-Rad53p immunoblotting to monitor phospho-electrophoretic mobility variants of Rad53p. (B) Pds1p degradation. *cdc14-1* (MLY181) and *cdc14-1 ulp2*Δ (MLY183) *PDS1-myc* strains were grown to logarithmic phase at 23°C and then washed into media containing either 0.001%, 0.005%, or 0.01% MMS. After a 2 hr MMS treatment, cells were washed into MMS-free media (0 time point) and shifted to 35°C to inactivate *cdc14-1*, thereby blocking mitotic exit after cells recovered from MMS. Protein extracts were prepared at the indicated times, protein concentrations were quantified, and equal amounts of protein were fractionated on SDS-PAGE gels. Pds1p-myc abundance was examined by α-myc immunoblotting. Ponceau staining was used to confirm equivalency of protein load (not shown). A protein sample from a mid-logarithmic phase culture of a WT strain (CRY1) was used as a no-tag control. (C) The gel analysis tools of NIH Image J were used to quantify the Pds1p bands shown in (B). Values were normalized to the 0 time point and expressed as a percent. WT (squares); *ulp2*Δ (circles).
doi:10.1371/journal.pgen.1001355.g005

in HU treated WT cells [56], consistent with an underlying replication problem in *ulp2*Δ mutants that is exacerbated by slowed fork progression.

In analyzing genome stability in *ulp2*Δ strains, we observed two interesting differences compared to other SUMO pathway mutants. First, whereas our data indicate that Rad6p-dependent PRR is essential in *ulp2* mutants, mis-regulation of SUMO conjugation in *ulp1-I165N rad18* [47], *ubc9-1 rad18* [19], *siz1 rad18* [11], *pol30-K164R rad18* and *pol30-K164R rad6* [5] mutants can actually compensate for defective PRR. One scenario that might account for this difference is if poly-sumoylation of a Ulp2p substrate(s) caused a distinct perturbation to DNA replication that was repaired through PRR-mediated HR. In keeping with this interpretation, we find that blocking poly-SUMO chain formation reduces the accumulation of both spontaneous and MMS-induced HR foci in *ulp2*Δ mutants.

A second apparent difference concerns the formation of GCRs. In contrast to *smt3-331*, *ubc9-1* and *ulp1-333* strains, where spontaneous GCRs are increased, *ulp2*Δ mutants show reduced GCRs. Formally, Ulp2p could promote GCR formation by stimulating error prone DNA repair. There is precedence for this, as a previous study found that, in the absence of template switch PRR, Siz1p-mediated sumoylation of PCNA was required to form certain types of GCRs [66]. Alternatively, Ulp2p could be required for cells that would give rise to GCRs to recover and propagate efficiently. Our observations with dicentric minichromosomes are consistent with the idea that repair events leading to some GCRs may not be tolerated in *ulp2*Δ strains. We were able to recover re-arranged dicentrics from *ulp2*Δ mutants when duplicated *CEN* sequences were present in a direct repeat configuration. Such deletions can occur through single-strand annealing, an intra-chromosomal form of recombination [67]. In contrast, *CEN* deletion GCRs were not recovered when the two *CENs* were oriented as inverted repeats. Recent studies have shown that faulty template switch PRR is frequently involved in initiating deletions between inverted repeats [68,69]. As discussed below, one possibility is that such recombination events are accompanied by formation of SCJs or other types of chromatid attachments that fail to be resolved in *ulp2* cells.

Ulp2p prevents accumulation of HR intermediates

Our results led us to suspect that HR DNA repair, while required for viability, might at the same time be toxic to *ulp2* cells, prompting us to examine processing of MMS-induced recombination events. From this analysis, one conclusion is that, similar to Ubc9p, Mms21p, Smc5p/Smc6p, and Sgs1p/Top3p [17,19], Ulp2p is required to prevent X-shaped DNA structures from accumulating at sites of replication fork stalling/collapse. We also find that, whereas Rad52p foci disappear during MMS recovery in WT cells, the incidence of these foci remains elevated in *ulp2*Δ strains, suggesting a possible role for Ulp2p in terminating recombination. Determining the molecular basis for how Ulp2p prevents accumulation of HR intermediates, and whether this

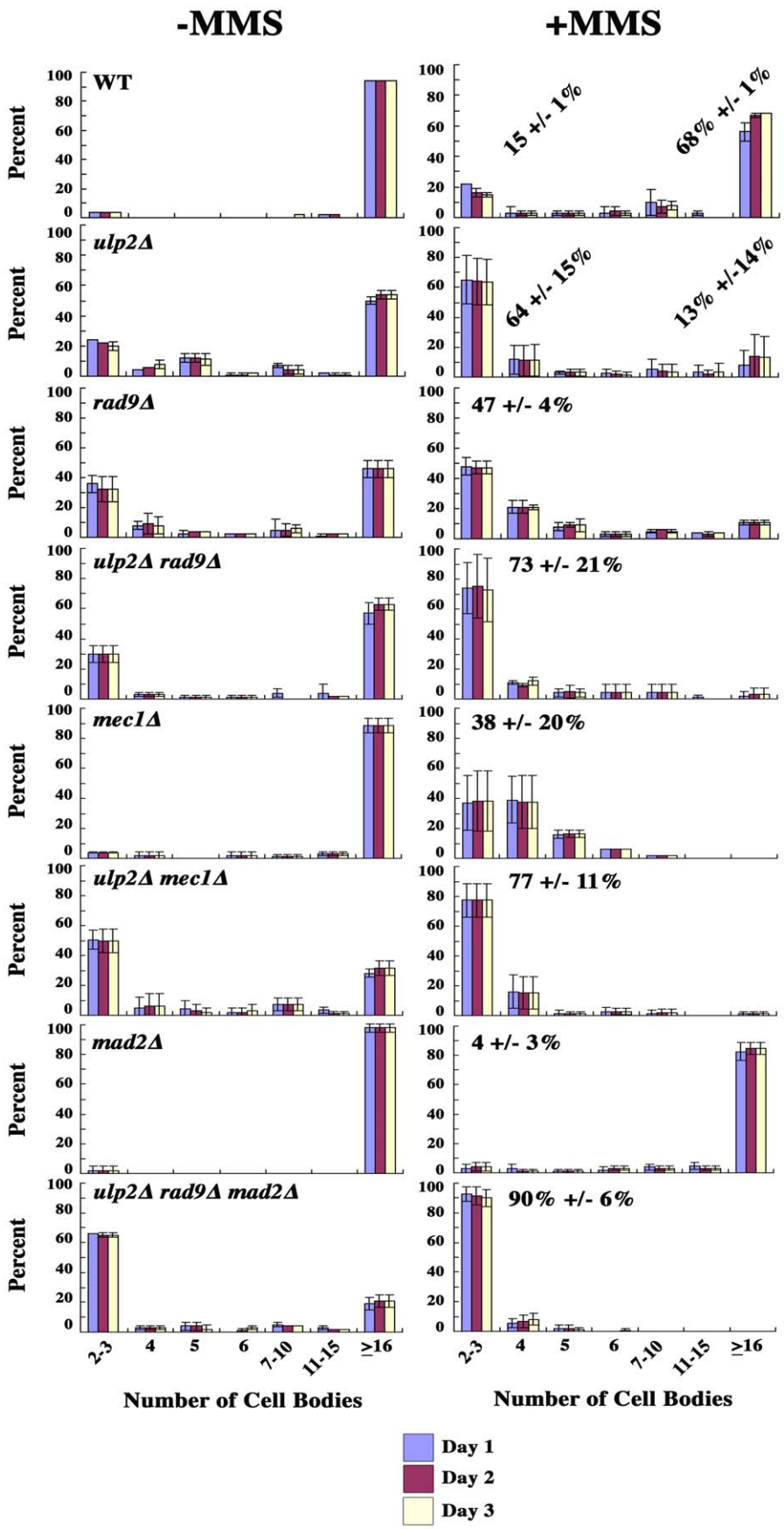
-MMS
+MMS
WT
ulp2Δ
rad9Δ
ulp2Δ rad9Δ
mec1Δ
ulp2Δ mec1Δ
mad2Δ
ulp2Δ rad9Δ mad2Δ
15 +/- 1%
68% +/- 1%
64 +/- 15%
13% +/-14%
47 +/- 4%
73 +/- 21%
38 +/- 20%
77 +/- 11%
4 +/- 3%
90% +/- 6%
Percent
2-3
4
5
6
7-10
11-15
≥16
Number of Cell Bodies
Day 1
Day 2
Day 3

Figure 6. Microcolony analysis of MMS–treated *ulp2*Δ mutants. Cultures of WT (MLY061), *ulp2*Δ (MLY060), *rad9*Δ (MLY112), *ulp2*Δ *rad9*Δ (MLY064), *mec1*Δ *GAP-RNR3* (JBY321; *MEC1* essential function provided by overproduction of Rnr3p, [86]), *ulp2*Δ *mec1*Δ *GAP-RNR3* (MLY108), *mad2*Δ (JBY554), and *ulp2*Δ *rad9*Δ *mad2*Δ (MLY160) strains were split, and half the cultures was treated with 0.01% MMS for 2 hr. For both treated (+MMS) and untreated (−MMS) cultures, 50 large-budded cells (equivalent to 2 cell bodies) were micro-manipulated onto a grid pattern on a YPD plate, and the number of cell bodies in the resulting micro-colonies were monitored over the next 3 days. The graphs display the average of three separate experiments for each strain, ± one standard deviation. Numbers on the +MMS graphs indicate the average percent of cells that remain blocked with 2–3 cell bodies. For the WT and *ulp2*Δ strains, the average percentage of cells capable of recovering to form microcolonies of ≥ 16 cell bodies is also indicated.
doi:10.1371/journal.pgen.1001355.g006

function is related to or separate from Ulp2p's role in Rad52p foci disassembly, are important future questions.

Based on current information, Ulp2p could be connected to HR through a number of different SUMO substrates. First, Mms21p-mediated sumoylation of unknown substrates, probably in conjunction with Smc5p/Smc6p [22,70], has been proposed to prevent excessive template switch recombination through PRR [19]. Alternatively, more recent evidence suggests Smc5p/Smc6p may instead act downstream of PRR to facilitate the dissolution of HR intermediates [71]. Second, Sgs1p is sumoylated under conditions when it is active in SCJ dissolution [17,59], although apparently through an Mms21-independent pathway [17]. Third, Ubc9p/Siz1p-controlled sumoylation of PCNA and recruitment of Srs2p may suppress PRR-independent recombination at replication forks [6,7,19]. Fourth, Srs2p has also been shown to be sumoylated, with poly-sumoylation being proposed to trigger Srs2p degradation through the Slx5p/Slx8p pathway [72]. Fifth, a fraction of Rad52p [73-75], and other HR proteins [76], are sumoylated in response to MMS, which may be involved in fine-tuning processing of broken DNA. Finally, a growing number of protein-protein interactions within HR foci have been found to be controlled by sumoylation (reviewed in [77]). As part of completion of repair, Ulp2p may catalyze the disassembly of these networks.

As a first step in placing Ulp2p in these pathways, we tested whether mis-regulation of Sgs1p sumoylation was connected to *ulp2*Δ HR defects. Overproduction of Ulp2p was recently shown to block Sgs1p sumoylation on K621 following MMS treatment [59], and, as we report here, MMS-induced sumoylation of Sgs1p is elevated in the absence of Ulp2p. It is therefore likely that Ulp2p acts as the SUMO deconjugating enzyme for Sgs1p. Despite this, short-circuiting Sgs1p sumoylation using the *sgs1-K621R* mutation

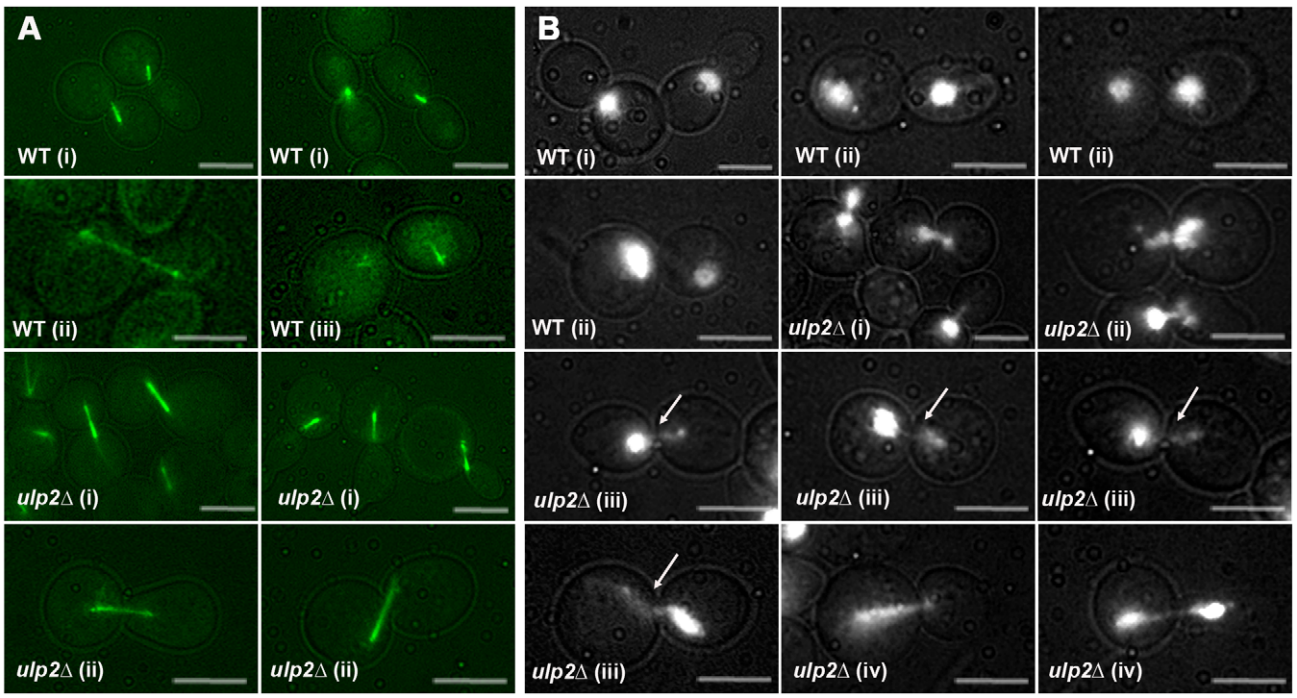

Figure 7. Chromosome segregation failure in MMS–treated *ulp2*Δ mutants. (A) Imaging spindle morphology using GFP-tagged tubulin. WT (JBY431) and *ulp2*Δ (JBY448) *TUB1-GFP* strains were treated with 0.01% MMS for 2 hr and washed into MMS-free media. After a 4–6 hr recovery, live cell mounts were imaged with low-level bright field illumination and for fluorescence. Scale bar in all cases is 4 μm. These strains also harbor a LacO/LacI-GFP chromosome tag (*TRP1-GFP*) that is visible in some images. *WT micrographs*. (i) Normal pre-anaphase spindles. (ii) Anaphase spindle extension after recovery. (iii) Spindle disassembly following completion of chromosome segregation. *ulp2*Δ *micrographs*. (i) Partial or incomplete spindle extension observed in many *ulp2*Δ cells. (ii) Higher magnification of partial spindle extension. (B) Imaging chromatin using YFP-tagged histone H2 (Hhf2p-YFP). A *ulp2*Δ/+ *HHF2-YFP*/+ diploid strain (JBY1806) was sporulated to generate WT *HHF2-YFP* and *ulp2*Δ *HHF2-YFP* haploid segregants, which were treated with MMS, allowed to recovery, and imaged as in (A). Scale bars, 4 μm. *WT micrographs*. (i) Pre-anaphase cells with a single undivided nucleus. (ii) Cells that have recovered and completed nuclear segregation. *ulp2*Δ *micrographs*. (i and ii) During recovery, many *ulp2*Δ cells exhibited an irregular, bi-lobed chromatin morphology; examples at 60X and 100X, respectively. (iii) Examples of cells with thin chromatin filaments (arrows) extending from a main focus of unsegregated chromatin. (iv) *ulp2*Δ cells displaying more extensive chromosome separation and chromatin stretching along the spindle; the cell in the right panel would be scored as having undergone nuclear segregation.
doi:10.1371/journal.pgen.1001355.g007

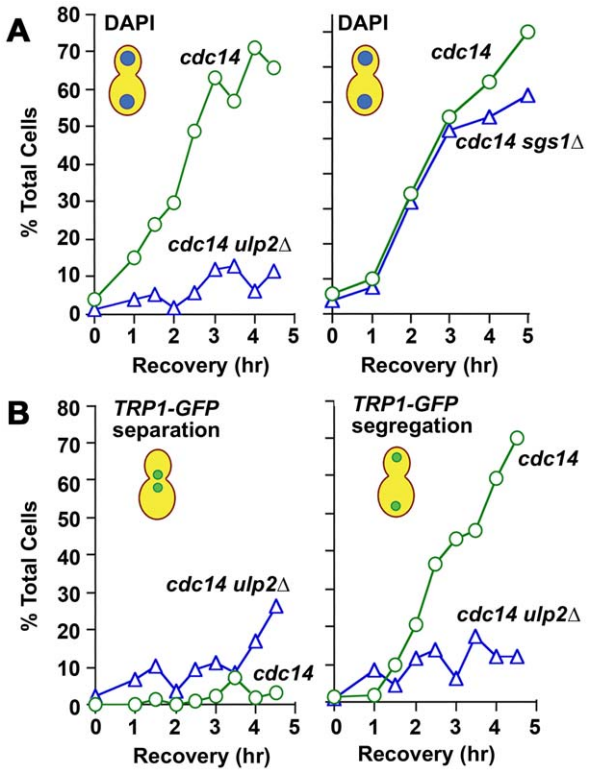

Figure 8. Chromosome disjunction in MMS–treated *ulp2*Δ mutants. (A) Bulk chromosome separation. *cdc14-1* (MLY181, JBY531; circles), *cdc14-1 ulp2*Δ (MLY183, triangles in left graph), and *cdc14-1 sgs1*Δ (JBY1809, triangles in right graph) strains were cultured at 23°C, treated with 0.01% MMS for 2 hr, and allowed to recover (0 time point) at 35°C to inactivate *cdc14-1*. At the indicated times, samples were fixed, stained with DAPI, and scored for binucleate cells indicative of successful nuclear division. ≥ 100 cells were scored per time point. (B) Chromosome separation and segregation at *TRP1-GFP*. *cdc14-1* (JBY642, circles) and *cdc14-1 ulp2*Δ (JBY643, triangles) *TRP1-GFP* strains were treated with MMS and allowed to recover as in (A). At the indicated times, cells were fixed and scored for *TRP1-GFP* disjunction (two distinct, separated *TRP1-GFP* foci) and segregation (separated *TRP1-GFP* foci that have been partitioned between mother and daughter cells). ≥ 50 cells were scored for each time point.
doi:10.1371/journal.pgen.1001355.g008

did not reduce Rad52p foci accumulation in *ulp2*Δ cells, indicating mis-regulation of other Ulp2p substrates is likely to be involved in modulating HR.

HR and the *ulp2* recovery defect

The failure of *ulp2* mutants to resume cell division following DNA damage is one of the most intriguing aspects of the *ulp2* phenotype. The first study to document this phenomenon showed that, following adaptation to a persistent DNA break, only a fraction of *ulp2* cells were able to proceed with nuclear division, frequently accompanied by abnormally extended or broken mitotic spindles [41]. Inactivating the DNA damage checkpoint rescued this defect, suggesting a critical role for Ulp2p in re-initiating chromosome segregation following completion of the checkpoint response [41,48].

While our results are largely in accord with this study, we observed a potentially informative difference in the role of the checkpoint in manifesting the *ulp2*Δ recovery defect. During MMS recovery, *ulp2*Δ cells dephosphorylated Rad53p and degraded Pds1p on schedule, suggesting they were competent to silence the checkpoint and initiate anaphase. Despite this, sister chromatids failed to disjoin, resulting in a dramatic failure in chromosome segregation. OP of Srs2p, which antagonizes HR [8-10,63,64], was able to largely restore chromosome segregation. In addition to modulating nucleo-protein filament assembly, Srs2p has also been shown to be required for full activation of the DNA damage checkpoint and for recovery from DNA damage checkpoint arrest [78,79]. In our experiments, we observed that Srs2p OP greatly extended DNA damage checkpoint arrest in MMS treated WT cells. Based on the above considerations, this extended arrest could presumably reflect either mis-regulation of the checkpoint pathway, or, by interfering with HR DNA repair, elevated Srs2p could simply prolong normal checkpoint signaling. While the effects of Srs2 OP on checkpoint signaling and HR may be multi-faceted, the key point we wish to emphasize here is that abolishing the DNA damage checkpoint (or the SAC) did not allow *ulp2*Δ cells to divide more times during recovery from MMS treatment. Furthermore, preventing DNA damage checkpoint arrest in MMS treated *ulp2*Δ *rad9*Δ cells was insufficient to relieve the block to chromosome separation; OP of Srs2 was also necessary. In sum, these findings strongly suggest that, following replication fork stalling by MMS, downstream events initiated through HR, rather than checkpoint arrest *per se*, appear to play a causal role in interfering with chromosome segregation.

A key question concerns how HR could have this effect. Perhaps the simplest idea is that unresolved SCJs block chromatid disjunction. Whether this is a sufficient explanation, however, is unclear. First, in the experiments examining *ulp2* adaptation to a persistent, endonuclease-targeted DNA break, both chromatids would be expected to be cut, preventing HR strand exchange [41]. Thus, the only way in which DNA linkages could form between chromosomes in these cells would be if extensive resection during prolonged checkpoint arrest triggered illegitimate recombination events. Second, we show that MMS treated *sgs1*Δ mutants, which are clearly defective in the dissolution of SCJs [17,25,27], do not show as severe a block to chromosome separation as Ulp2p-deficient cells. This is consistent with a recent study that showed, from among a collection of helicase-, nuclease-, and topoisomerase-deficient mutants, only *smc5*, *smc6* and *mms21* strains showed chromosome segregation defects after a pulse of MMS delivered in G1 [71]. This suggests a role for Mms21p-mediated sumoylation and the Smc5p/Smc6p complex in resolving SCJs or other types of chromatid linkages outside the Sgs1p/Top3p pathway [71]. Along these lines, it is notable that Ulp2p has been implicated in multiple facets of chromatid separation, including controlling sumoylation of cohesin regulatory proteins [37,42], condensin [35,38], and DNA topoisomerase II [36,40]. Speculatively, following induction of HR, there may be an increased requirement for Ulp2p in the vicinity of DNA lesions, not only to prevent accumulation of HR intermediates, but also to complete replication, to disentangle DNA or to release protein-based forms of cohesion. Given the dramatic way in which the absence of Ulp2p potentiates the ability of replication toxins to block cell proliferation, a further understanding of the *ulp2* recovery defect could lead to insights that are relevant to cancer treatment.

Materials and Methods

Yeast strains and culture

All *S. cerevisiae* strains used in this study were derived from the W303-related CRY1 strain and are listed in Table S1. A description of how different genetic elements were introduced into the CRY1 background can be found in Text S1. For all experiments, cells were cultured in standard formulations of yeast

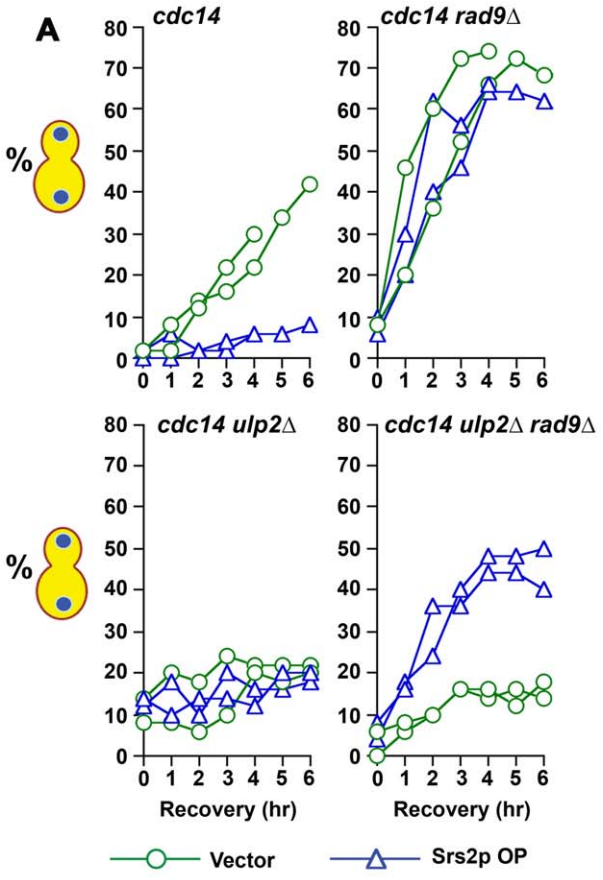

Figure 9. Effect of Srs2p OP and inactivating the DNA damage checkpoint on chromosome segregation during MMS recovery. *cdc14-1* (MLY181), *cdc14-1 rad9*Δ (MLY186), *cdc14-1 ulp2*Δ (MLY183), and *cdc14-1 ulp2*Δ *rad9*Δ (MLY189) strains were transformed with a vector control (pRS426; [84]) or a high copy plasmid expressing *SRS2* under control of its endogenous promoter (p*SRS2*; YEplac195-*SRS2*; [85]). Transformants were cultured under selection for the plasmid at 23°C, treated with 0.01% MMS for 2 hrs, and allowed to recover (0 time point) at 35°C to inactivate *cdc14-1*. (A) Cell aliquots were removed at the indicated times, stained with DAPI, and scored for nuclear segregation. Graphs display results from two separate experiments; vector transformants (circles); Srs2 OP transformants (triangles). For one experiment, *cdc14-1* and *cdc14-1 rad9*Δ strains were only scored to 4 hr. (B) Representative images of *cdc14-1 ulp2*Δ *rad9*Δ/vector cells with undivided nuclei and examples of *cdc14-1 ulp2*Δ *rad9*Δ/p*SRS2* cells that would be scored as having completed chromosome segregation. All images taken 4 hr post-treatment. Scale bar, 4 μm.
doi:10.1371/journal.pgen.1001355.g009

extract/peptone/dextrose (YPD) and synthetic complete minimal (SC) media. For G1 synchronization, alpha factor (Bio-Synthesis Corp.) was used at 10 μg/ml. For arresting cells in G2/M, nocodazole (Sigma-Aldrich) was used at 15 μg/ml in YPD. MMS and HU were purchased from Sigma-Aldrich. 5-FOA was purchased from Biovectra/Fisher and used at 1 mg/ml. G418 was purchased from Mediatech/Fisher and used at 200 μg/ml in YPD.

Recombination frequency

pLAY202 ([50]; provided by A. Bailis, City of Hope National Medical Center, Duarte, CA) was linearized with BstXI and targeted to the *HIS3* locus, placing a *URA3* marker between partially duplicated *HIS3* sequences. pLAY202 integrants were propagated in Ura$^-$/SC media, and, following overnight incubation, cell density was quantified using a hemacytometer. Viable cell counts were determined by plating a defined number of cells onto YPD and counting the resulting colonies. Recombination events were selected by plating a larger number of cells onto His$^-$/SC media, and replica plating colonies that arose onto 5-FOA. Colonies that reverted to a His$^+$, Ura$^-$ phenotype were scored as recombinants.

GCR frequency

YAC yWss1572-1 ([53]; provided by D. Koshland, Univ. of California at Berkeley, Berkeley, CA) was modified so that the *TRP1* marker on the left arm of the YAC was replaced with *kanMX*. This was performed by PCR amplifying a *trp1*Δ::*kanMX* disruption cassette using the following primers

5′-GCATATAAAAATAGTTCAGGCACTCCGAAATACT-TGGTTGGCGTGTTTC

GTCAGCTGAAGCTTCGTACGC (CO354)

5′-TCTGGCGTCAGTCCACCAGCTAACATAAAATGTA-AGCTTTCGGGGCGCAT

AGGCCACTAGTGGATCTG (CO355)

and pFA6a/*kanMX2* [80] as template. G418^{Res}, Trp$^-$ transformants were analyzed by PCR to verify correct targeting. The resulting YAC, named yWss1572Δ*trp1*, was subsequently transferred between strains using cytotransduction [81] or standard genetic crosses. To isolate GCRs, strains containing yWss1572Δ*trp1* were grow in Ura$^-$/SC media at 30°C for WT, *ulp2*Δ, *ubc9-1* and *smt3-331* strains, and 34°C for *ulp1-333* mutants; these represent semi-permissive temperatures for the *ubc9-1*, *smt3-331* and *ulp1-333* alleles. Cell densities were quantified using a hemacytometer, and dilutions of the cultures were plated onto YPD to monitor plating efficiency. Aliquots of 10^5, 10^6, 10^7 and

10^8 cells were plated on 5-FOA to select for loss of the *URA3* marker on the YAC. Colonies arising on 5-FOA were replica plated to YPD/G418 and Ade$^-$/SC media. Clones growing on 5-FOA and YPD/G418, but not on Ade$^-$/SC (G418^{Res}, 5-FOA^{Sen}, Ade$^-$) were considered to arise from GCRs deleting the right arm of the YAC. In contrast, clones that were able to grow on 5-FOA, but could not grow on YPD/G418 or Ade$^-$/SC (G418^{Sen}, 5-FOA^{Sen}, Ade$^-$) were considered to arise through YAC mis-segregation events. For each culture, the total number of GCR clones arising on all the assay plates was used to calculate GCR frequency.

Minichromosome loss

To monitor the mitotic stability of dicentric minichromosomes, p2X*CEN*^{direct} (pJBN152; a YRp14-derived minichromosome containing two copies of a 1.7 kb *CEN1* DNA fragment in a direct repeat configuration, see Text S1) and p2X*CEN*^{invert} (pJBN151; similar to pJBN152 but with the *CEN1* duplication oriented as an inverted repeat) were transformed into WT and *ulp2*Δ strains and compared to p1X*CEN* (YRp14/*CEN1*) controls. Transformants were inoculated into parallel YPD and Ura$^-$/SC cultures and incubated at 30°C. After ~15 hr of outgrowth, appropriate dilutions were plated onto YPD and Ura$^-$/SC media. Mitotic stability was calculated by dividing the number of Ura$^+$ colonies by the total number of colonies obtained on YPD.

Microscopy and flow cytometry

Cultures for microscopy were supplemented with 50 μg/ml adenine to quench auto-fluorescence. To visualize Rad52p-GFP and *TRP1-GFP*, cells were fixed in 1% formaldehyde for 1.5 min and washed into PBS. DAPI staining was performed using Vecta-Shield (Vector Laboratories) containing 10 μg/ml DAPI. *TUB1-GFP* and *HHF2-YFP* strains were visualized as live mounts. *HHF2-YFP* is typically propagated as a heterogyzous diploid (*HHF2-YFP-HIS3*/+) to minimize selective pressure for rearranged variants that lose the fluorescent marker. However, in order to compare the response of *HHF2-YFP* strains to MMS concentrations similar to those used in our other recovery experiments, we chose to examine *HHF2-YFP* haploid segregants that were generated on an experiment-by-experiment basis. This proved to allow propagation of haploid strains with robust Hhf2-YFP fluorescence. In all cases, cells were visualized on Nikon E-800 or Nikon Eclipse 80i microscopes equipped with florescence optics and 100X (1.4 NA) or 60X (1.4 NA) objectives. Rad52p-GFP foci were typically scored using a number 4 neutral density filter to minimize photobleaching. A Zeiss Axioskop 40 microscope equipped with a 25 μm diameter optical fiber dissection needle was used to micromanipulate yeast cells for microcolony analysis. FACS analysis was performed by staining ethanol fixed yeast cells with propidium iodide as previously described [82].

Pulse field gel electrophoresis

10 ml aliquots of OD_{600} 0.8 cultures were harvested by centrifugation and concentrated into 400 μl cell suspension buffer (10 mM Tris, 20 mM NaCl, 50 mM EDTA, pH 7.2). The cell suspension was warmed to 55°C and mixed with 400 μl 2% low melting temperature agarose (SeaKem) dissolved in TBE gel electrophoresis buffer (kept molten at 55°C) containing lyticase (Sigma L4025; final concentration 1 mg/ml). The cell suspension was transferred into molds and allowed to solidify to form plugs (4°C, 15 min). Plugs were pushed out into 50 ml conical tubes and incubated with 5 ml 1 mg/ml lyticase dissolved in 10 mM Tris, 50 mM EDTA, pH 7.2 for one hr at 37°C, followed by treatment 1 mg/ml Proteinase K (Sigma) dissolved in 100 mM EDTA, 0.2% Na Deoxycholate, 1% Na lauryl sarcosine, pH 8.0 at 50°C overnight. Plugs were washed (20 mM Tris, 50 mM EDTA, pH 8.0) 4 times one hour each and stored in wash buffer. Prior to electrophoresis, plugs were placed on a glass plate and trimmed to fit electrophoresis wells. Samples were then fractionated on 1% agarose gels in TBE using a Bio-Rad CHEF-DR II pulsed field electrophoresis system at 6V/cm for 22 hrs with a switch ramp time ramped from 50 to 90 sec at 14°C. Gels were stained with ethidium bromide (0.5 μg/ml, 15 min) prior to photography.

Two-dimensional gel analysis

Genomic DNA preparations and two-dimensional gel electrophoresis were performed according to detailed online methods available from the Brewer-Raghuraman laboratory:

(http://fangman-brewer.genetics.washington.edu/DNA_prep.html)

(http://fangman-brewer.genetics.washington.edu/2Dgel.html)

In brief, cells were grown in 500 ml YPD until the cultures reached an OD_{600} of 0.6. The cultures were synchronized in nocodazole for 2 hr, washed, and released into fresh YPD containing 0.033% MMS. After a 3 hr treatment, cells were harvested by centrifugation and stored in 5 ml of NIB buffer (17% glycerol, 50 mM MPOS free acid, 150 mM potassium acetate, 2 mM magnesium chloride, 150 μM spermine and 500 μM spermidine, pH 7.2). Cells were lysed by bead beating in NIB buffer, and genomic DNA was purified on cesium chloride density gradients. The resulting DNA samples were digested with HindIII and EcoRV. For first dimension separation, ~30 μg of digested DNA was loaded onto 0.35% agarose gels and fractionated at 22 volts for 42–48 hr at room temperature. Gel slices containing DNA in the 3–10 kb range were excised and positioned onto a 0.95% agarose gel. Electrophoresis in the second dimension was performed at 4°C at 80 volts for 17 hr at room temperature and 130 volts for another 1.5 hr. Following transfer to nylon membranes (Hybond-XL, GE Healthcare), samples were hybridized with a 280 bp ARS305 DNA fragment PCR amplified from genomic DNA using the following primers:

5′-CTCCGTTTTTAGCCCCCCGTG-

5′-GATTGAGGCCACAGCAAGACCG

The PCR product was radio-labeled (Megaprime DNA labeling system, GE Healthcare) and hybridized using Southern blot procedures as previously described [83].

Protein techniques

Protein extracts were prepared by mechanical beakage of cells in 20% TCA as previously described [36]. 6% SDS-PAGE gels were used to fractionate samples for analysis of Sgs1p-myc and Pds1p-myc, while 12% SDS-PAGE gels (acrylamide: bis = 30:0.39) were used to analyze phosphorylated species of Rad53p. α-myc (9E10, 1:1000, Covance), α-Rad53p (SC-6749, 1:2000, Santa Cruz), and HRP conjugated secondary (1:25,000; Jackson ImmunoResearch) antibodies were used for immunoblotting.

Supporting Information

Figure S1 Analysis of Sgs1p SUMO conjugation. A sgs1Δ mutant strain (MLY200) was transformed with plasmids encoding untagged SGS1 (no tag; YCplac33/SGS1), SGS1-18Xmyc (pJBN276), or the sgs1-K621R-18Xmyc mutant allele (pJBN277). Duplicate cultures of these transformants were treated with 0.03% MMS for 2 hrs or were maintained in MMS-free media, and protein samples were analyzed by α-myc immunoblotting. As observed previously [11], a shifted form of Sgs1p is observed in

MMS-treated SGS1 transformants but not in cells transformed with the sgs1-K621R allele.
Found at: doi:10.1371/journal.pgen.1001355.s001 (0.88 MB TIF)

Figure S2 Microcolonly analysis of MMS recovery in ulp2Δ mad2Δ mutants. In conjunction with the experiments shown in Figure 6, mid-logarithmic phase cultures of a ulp2Δ mad2Δ strain (JBY733) were split. One half was treated with 0.01% MMS for 2 hr while the other half was cultured for an equivalent period in MMS-free media. For both treated (+MMS) and untreated (−MMS) cultures, 50 large-budded cells (2 cell bodies) were micro-manipulated onto a grid pattern on a YPD plate, and the number of cell bodies in the resulting micro-colonies were monitored over 3 days. The graphs display the average from three separate experiments, ± one standard deviation. The average percent of MMS treated cells that remain blocked with 2–3 cell bodies is indicated.
Found at: doi:10.1371/journal.pgen.1001355.s002 (0.31 MB TIF)

Figure S3 FACS analysis of MMS treated ulp2Δ cells. WT (MLY061) and ulp2Δ (MLY060) strains were treated with 0.03% MMS for 2 hrs (−2 to 0 timepoints) and allowed to recover in MMS-free media. At the indicated times, samples were withdrawn and DNA content was examined by flow cytometry. Although ulp2Δ cells are blocked for chromosome segregation, they show an apparent increase in DNA content, suggesting that following this mitotic catastrophe they may attempt an addition round of DNA replication.
Found at: doi:10.1371/journal.pgen.1001355.s003 (0.81 MB TIF)

Figure S4 Chromosome segregation in MMS treated cdc14-1 sgs1Δ cells. cdc14-1 sgs1Δ RAD52-GFP cells (JBY1808) were cultured at 23°C, treated with 0.01% MMS for 2 hr, and allowed to recover at 35°C to inactivate cdc14-1. After a 5 hr recovery, aliquots were fixed, stained with DAPI, and imaged to visualize DNA and Rad52p-GFP foci. Micrographs depict cells in which chromosome separation and nuclear segregation are largely complete, but with faint DAPI-staining fibers that appear to connect the nuclei. Persistent Rad52p-GFP foci are often observed in these cells. In some cases the Rad52p-GFP foci appear to co-localize on the DAPI-staining fibers, while in others the foci appear to have partitioned with the bulk of chromosomal DNA. BLM-deficient human cells (BLM is the human homologue of Sgs1) exposed to replication stress have been shown to accumulate ultra-fine sister chromatid bridges that are thought to arise from unresolved DNA linkages [12]. Speculatively, MMS treated sgs1Δ cells may form similar types of structures.
Found at: doi:10.1371/journal.pgen.1001355.s004 (2.40 MB TIF)

Table S1 Yeast strains used in this study.
Found at: doi:10.1371/journal.pgen.1001355.s005 (0.13 MB DOC)

Text S1 Additional description of methods.
Found at: doi:10.1371/journal.pgen.1001355.s006 (0.27 MB DOC)

Acknowledgments

The authors wish to thank L. Xu and C. Nugent (University of California Riverside) for construction of the yWss1572Δ*trp1* YAC described in this study. Other colleagues who generously provided strains, plasmids, or other reagents are described in Text S1.

Author Contributions

Conceived and designed the experiments: MTL JB. Performed the experiments: MTL AAB KNN JB. Analyzed the data: MTL AAB KNN JB. Wrote the paper: MTL AAB KNN JB.

References

1. Broomfield S, Hryciw T, Xiao W (2001) DNA postreplication repair and mutagenesis in Saccharomyces cerevisiae. Mutat Res 486: 167–184.
2. San Filippo J, Sung P, Klein H (2008) Mechanism of eukaryotic homologous recombination. Annu Rev Biochem 77: 229–257.
3. Branzei D, Foiani M (2010) Maintaining genome stability at the replication fork. Nat Rev Mol Cell Biol 11: 208–219.
4. Johnson ES (2004) Protein modification by SUMO. Annu Rev Biochem 73: 355–382.
5. Hoege C, Pfander B, Moldovan GL, Pyrowolakis G, Jentsch S (2002) RAD6-dependent DNA repair is linked to modification of PCNA by ubiquitin and SUMO. Nature 419: 135–141.
6. Pfander B, Moldovan GL, Sacher M, Hoege C, Jentsch S (2005) SUMO-modified PCNA recruits Srs2 to prevent recombination during S phase. Nature 436: 428–433.
7. Papouli E, Chen S, Davies AA, Huttner D, Krejci L, et al. (2005) Crosstalk between SUMO and ubiquitin on PCNA is mediated by recruitment of the helicase Srs2p. Mol Cell 19: 123–133.
8. Krejci L, Van Komen S, Li Y, Villemain J, Reddy MS, et al. (2003) DNA helicase Srs2 disrupts the Rad51 presynaptic filament. Nature 423: 305–309.
9. Veaute X, Jeusset J, Soustelle C, Kowalczykowski SC, Le Cam E, et al. (2003) The Srs2 helicase prevents recombination by disrupting Rad51 nucleoprotein filaments. Nature 423: 309–312.
10. Antony E, Tomko EJ, Xiao Q, Krejci L, Lohman TM, et al. (2009) Srs2 disassembles Rad51 filaments by a protein-protein interaction triggering ATP turnover and dissociation of Rad51 from DNA. Mol Cell 35: 105–115.
11. Stelter P, Ulrich HD (2003) Control of spontaneous and damage-induced mutagenesis by SUMO and ubiquitin conjugation. Nature 425: 188–191.
12. Haracska L, Torres-Ramos CA, Johnson RE, Prakash S, Prakash L (2004) Opposing effects of ubiquitin conjugation and SUMO modification of PCNA on replicational bypass of DNA lesions in Saccharomyces cerevisiae. Mol Cell Biol 24: 4267–4274.
13. Kannouche PL, Wing J, Lehmann AR (2004) Interaction of human DNA polymerase eta with monoubiquitinated PCNA: a possible mechanism for the polymerase switch in response to DNA damage. Mol Cell 14: 491–500.
14. Maeda D, Seki M, Onoda F, Branzei D, Kawabe Y, et al. (2004) Ubc9 is required for damage-tolerance and damage-induced interchromosomal homologous recombination in S. cerevisiae. DNA Repair (Amst) 3: 335–341.
15. Andrews EA, Palecek J, Sergeant J, Taylor E, Lehmann AR, et al. (2005) Nse2, a component of the Smc5-6 complex, is a SUMO ligase required for the response to DNA damage. Mol Cell Biol 25: 185–196.
16. Zhao X, Blobel G (2005) A SUMO ligase is part of a nuclear multiprotein complex that affects DNA repair and chromosomal organization. Proc Natl Acad Sci U S A 102: 4777–4782.
17. Branzei D, Sollier J, Liberi G, Zhao X, Maeda D, et al. (2006) Ubc9- and mms21-mediated sumoylation counteracts recombinogenic events at damaged replication forks. Cell 127: 509–522.
18. van Waardenburg RC, Duda DM, Lancaster CS, Schulman BA, Bjornsti MA (2006) Distinct functional domains of Ubc9 dictate cell survival and resistance to genotoxic stress. Mol Cell Biol 26: 4958–4969.
19. Branzei D, Vanoli F, Foiani M (2008) SUMOylation regulates Rad18-mediated template switch. Nature 456: 915–920.
20. Onoda F, Takeda M, Seki M, Maeda D, Tajima J, et al. (2004) SMC6 is required for MMS-induced interchromosomal and sister chromatid recombinations in Saccharomyces cerevisiae. DNA Repair (Amst) 3: 429–439.
21. Torres-Rosell J, Machin F, Farmer S, Jarmuz A, Eydmann T, et al. (2005) SMC5 and SMC6 genes are required for the segregation of repetitive chromosome regions. Nat Cell Biol 7: 412–419.
22. Ampatzidou E, Irmisch A, O'Connell MJ, Murray JM (2006) Smc5/6 is required for repair at collapsed replication forks. Mol Cell Biol 26: 9387–9401.
23. Sollier J, Driscoll R, Castellucci F, Foiani M, Jackson SP, et al. (2009) The Saccharomyces cerevisiae Esc2 and Smc5-6 proteins promote sister chromatid junction-mediated intra-S repair. Mol Biol Cell 20: 1671–1682.
24. Karow JK, Constantinou A, Li JL, West SC, Hickson ID (2000) The Bloom's syndrome gene product promotes branch migration of holliday junctions. Proc Natl Acad Sci U S A 97: 6504–6508.
25. Liberi G, Maffioletti G, Lucca C, Chiolo I, Baryshnikova A, et al. (2005) Rad51-dependent DNA structures accumulate at damaged replication forks in sgs1 mutants defective in the yeast ortholog of BLM RecQ helicase. Genes Dev 19: 339–350.
26. Plank JL, Wu J, Hsieh TS (2006) Topoisomerase IIIalpha and Bloom's helicase can resolve a mobile double Holliday junction substrate through convergent branch migration. Proc Natl Acad Sci U S A 103: 11118–11123.
27. Mankouri HW, Ngo HP, Hickson ID (2007) Shu proteins promote the formation of homologous recombination intermediates that are processed by Sgs1-Rmi1-Top3. Mol Biol Cell 18: 4062–4073.

28. Li SJ, Hochstrasser M (1999) A new protease required for cell-cycle progression in yeast. Nature 398: 246–251.
29. Li SJ, Hochstrasser M (2000) The yeast ULP2 (SMT4) gene encodes a novel protease specific for the ubiquitin-like Smt3 protein. Mol Cell Biol 20: 2367–2377.
30. Schwienhorst I, Johnson ES, Dohmen RJ (2000) SUMO conjugation and deconjugation. Mol Gen Genet 263: 771–786.
31. Li SJ, Hochstrasser M (2003) The Ulp1 SUMO isopeptidase: distinct domains required for viability, nuclear envelope localization, and substrate specificity. J Cell Biol 160: 1069–1081.
32. Panse VG, Kuster B, Gerstberger T, Hurt E (2003) Unconventional tethering of Ulp1 to the transport channel of the nuclear pore complex by karyopherins. Nat Cell Biol 5: 21–27.
33. Kroetz MB, Su D, Hochstrasser M (2009) Essential role of nuclear localization for yeast Ulp2 SUMO protease function. Mol Biol Cell 20: 2196–2206.
34. Meluh PB, Koshland D (1995) Evidence that the MIF2 gene of Saccharomyces cerevisiae encodes a centromere protein with homology to the mammalian centromere protein CENP-C. Mol Biol Cell 6: 793–807.
35. Strunnikov AV, Aravind L, Koonin EV (2001) Saccharomyces cerevisiae SMT4 encodes an evolutionarily conserved protease with a role in chromosome condensation regulation. Genetics 158: 95–107.
36. Bachant J, Alcasabas A, Blat Y, Kleckner N, Elledge SJ (2002) The SUMO-1 isopeptidase Smt4 is linked to centromeric cohesion through SUMO-1 modification of DNA topoisomerase II. Mol Cell 9: 1169–1182.
37. Stead K, Aguilar C, Hartman T, Drexel M, Meluh P, et al. (2003) Pds5p regulates the maintenance of sister chromatid cohesion and is sumoylated to promote the dissolution of cohesion. J Cell Biol 163: 729–741.
38. D'Amours D, Stegmeier F, Amon A (2004) Cdc14 and condensin control the dissolution of cohesin-independent chromosome linkages at repeated DNA. Cell 117: 455–469.
39. Bachant J, Jessen SR, Kavanaugh SE, Fielding CS (2005) The yeast S phase checkpoint enables replicating chromosomes to bi-orient and restrain spindle extension during S phase distress. J Cell Biol 168: 999–1012.
40. Takahashi Y, Yong-Gonzalez V, Kikuchi Y, Strunnikov A (2006) SIZ1/SIZ2 control of chromosome transmission fidelity is mediated by the sumoylation of topoisomerase II. Genetics 172: 783–794.
41. Schwartz DC, Felberbaum R, Hochstrasser M (2007) The Ulp2 SUMO protease is required for cell division following termination of the DNA damage checkpoint. Mol Cell Biol 27: 6948–6961.
42. Baldwin ML, Julius JA, Tang X, Wang Y, Bachant J (2009) The yeast SUMO isopeptidase Smt4/Ulp2 and the polo kinase Cdc5 act in an opposing fashion to regulate sumoylation in mitosis and cohesion at centromeres. Cell Cycle 8: 3406–3419.
43. Bylebyl GR, Belichenko I, Johnson ES (2003) The SUMO isopeptidase Ulp2 prevents accumulation of SUMO chains in yeast. J Biol Chem 278: 44113–44120.
44. Uzunova K, Gottsche K, Miteva M, Weisshaar SR, Glanemann C, et al. (2007) Ubiquitin-dependent proteolytic control of SUMO conjugates. J Biol Chem 282: 34167–34175.
45. Tatham MH, Geoffroy MC, Shen L, Plechanovova A, Hattersley N, et al. (2008) RNF4 is a poly-SUMO-specific E3 ubiquitin ligase required for arsenic-induced PML degradation. Nat Cell Biol 10: 538–546.
46. Mullen JR, Brill SJ (2008) Activation of the Slx5-Slx8 ubiquitin ligase by poly-small ubiquitin-like modifier conjugates. J Biol Chem 283: 19912–19921.
47. Soustelle C, Vernis L, Freon K, Reynaud-Angelin A, Chanet R, et al. (2004) A new Saccharomyces cerevisiae strain with a mutant Smt3-deconjugating Ulp1 protein is affected in DNA replication and requires Srs2 and homologous recombination for its viability. Mol Cell Biol 24: 5130–5143.
48. Felberbaum R, Hochstrasser M (2008) Ulp2 and the DNA damage response: desumoylation enables safe passage through mitosis. Cell Cycle 7: 52–56.
49. Lisby M, Rothstein R, Mortensen UH (2001) Rad52 forms DNA repair and recombination centers during S phase. Proc Natl Acad Sci U S A 98: 8276–8282.
50. Maines S, Negritto MC, Wu X, Manthey GM, Bailis AM (1998) Novel mutations in the RAD3 and SSL1 genes perturb genome stability by stimulating recombination between short repeats in Saccharomyces cerevisiae. Genetics 150: 963–976.
51. Lambert S, Watson A, Sheedy DM, Martin B, Carr AM (2005) Gross chromosomal rearrangements and elevated recombination at an inducible site-specific replication fork barrier. Cell 121: 689–702.
52. Lemoine FJ, Degtyareva NP, Kokoska RJ, Petes TD (2008) Reduced levels of DNA polymerase delta induce chromosome fragile site instability in yeast. Mol Cell Biol 28: 5359–5368.
53. Huang D, Koshland D (2003) Chromosome integrity in Saccharomyces cerevisiae: the interplay of DNA replication initiation factors, elongation factors, and origins. Genes Dev 17: 1741–1754.
54. Mann C, Davis RW (1983) Instability of dicentric plasmids in yeast. Proc Natl Acad Sci U S A 80: 228–232.
55. Koshland D, Rutledge L, Fitzgerald-Hayes M, Hartwell LH (1987) A genetic analysis of dicentric minichromosomes in Saccharomyces cerevisiae. Cell 48: 801–812.
56. Barlow JH, Rothstein R (2009) Rad52 recruitment is DNA replication independent and regulated by Cdc28 and the Mec1 kinase. Embo J 28: 1121–1130.
57. Zou H, Rothstein R (1997) Holliday junctions accumulate in replication mutants via a RecA homolog-independent mechanism. Cell 90: 87–96.
58. Lopes M, Cotta-Ramusino C, Liberi G, Foiani M (2003) Branch migrating sister chromatid junctions form at replication origins through Rad51/Rad52-independent mechanisms. Mol Cell 12: 1499–1510.
59. Lu CY, Tsai CH, Brill SJ, Teng SC (2010) Sumoylation of the BLM ortholog, Sgs1, promotes telomere-telomere recombination in budding yeast. Nucleic Acids Res 38: 488–498.
60. Sanchez Y, Desany BA, Jones WJ, Liu Q, Wang B, et al. (1996) Regulation of RAD53 by the ATM-like kinases MEC1 and TEL1 in yeast cell cycle checkpoint pathways. Science 271: 357–360.
61. Cohen-Fix O, Peters JM, Kirschner MW, Koshland D (1996) Anaphase initiation in Saccharomyces cerevisiae is controlled by the APC-dependent degradation of the anaphase inhibitor Pds1p. Genes Dev 10: 3081–3093.
62. Cohen-Fix O, Koshland D (1997) The anaphase inhibitor of Saccharomyces cerevisiae Pds1p is a target of the DNA damage checkpoint pathway. Proc Natl Acad Sci U S A 94: 14361–14366.
63. Dupaigne P, Le Breton C, Fabre F, Gangloff S, Le Cam E, et al. (2008) The Srs2 helicase activity is stimulated by Rad51 filaments on dsDNA: implications for crossover incidence during mitotic recombination. Mol Cell 29: 243–254.
64. Prakash R, Satory D, Dray E, Papusha A, Scheller J, et al. (2009) Yeast Mph1 helicase dissociates Rad51-made D-loops: implications for crossover control in mitotic recombination. Genes Dev 23: 67–79.
65. Xiong L, Chen XL, Silver HR, Ahmed NT, Johnson ES (2009) Deficient SUMO attachment to Flp recombinase leads to homologous recombination-dependent hyperamplification of the yeast 2 microm circle plasmid. Mol Biol Cell 20: 1241–1251.
66. Motegi A, Kuntz K, Majeed A, Smith S, Myung K (2006) Regulation of gross chromosomal rearrangements by ubiquitin and SUMO ligases in Saccharomyces cerevisiae. Mol Cell Biol 26: 1424–1433.
67. Fishman-Lobell J, Rudin N, Haber JE (1992) Two alternative pathways of double-strand break repair that are kinetically separable and independently modulated. Mol Cell Biol 12: 1292–1303.
68. Paek AL, Kaochar S, Jones H, Elezaby A, Shanks L, et al. (2009) Fusion of nearby inverted repeats by a replication-based mechanism leads to formation of dicentric and acentric chromosomes that cause genome instability in budding yeast. Genes Dev 23: 2861–2875.
69. Mizuno K, Lambert S, Baldacci G, Murray JM, Carr AM (2009) Nearby inverted repeats fuse to generate acentric and dicentric palindromic chromosomes by a replication template exchange mechanism. Genes Dev 23: 2876–2886.
70. Irmisch A, Ampatzidou E, Mizuno K, O'Connell MJ, Murray JM (2009) Smc5/6 maintains stalled replication forks in a recombination-competent conformation. Embo J 28: 144–155.
71. Bermudez-Lopez M, Ceschia A, de Piccoli G, Colomina N, Pasero P, et al. (2010) The Smc5/6 complex is required for dissolution of DNA-mediated sister chromatid linkages. Nucleic Acids Res.
72. Saponaro M, Callahan D, Zheng X, Krejci L, Haber JE, et al. (2010) Cdk1 targets Srs2 to complete synthesis-dependent strand annealing and to promote recombinational repair. PLoS Genet 6: e1000858. doi:10.1371/journal.pgen.1000858.
73. Sacher M, Pfander B, Hoege C, Jentsch S (2006) Control of Rad52 recombination activity by double-strand break-induced SUMO modification. Nat Cell Biol 8: 1284–1290.
74. Torres-Rosell J, Sunjevaric I, De Piccoli G, Sacher M, Eckert-Boulet N, et al. (2007) The Smc5-Smc6 complex and SUMO modification of Rad52 regulates recombinational repair at the ribosomal gene locus. Nat Cell Biol 9: 923–931.
75. Ohuchi T, Seki M, Branzei D, Maeda D, Ui A, et al. (2008) Rad52 sumoylation and its involvement in the efficient induction of homologous recombination. DNA Repair (Amst) 7: 879–889.
76. Burgess RC, Rahman S, Lisby M, Rothstein R, Zhao X (2007) The Slx5-Slx8 complex affects sumoylation of DNA repair proteins and negatively regulates recombination. Mol Cell Biol 27: 6153–6162.
77. Bergink S, Jentsch S (2009) Principles of ubiquitin and SUMO modifications in DNA repair. Nature 458: 461–467.
78. Liberi G, Chiolo I, Pellicioli A, Lopes M, Plevani P, et al. (2000) Srs2 DNA helicase is involved in checkpoint response and its regulation requires a functional Mec1-dependent pathway and Cdk1 activity. Embo J 19: 5027–5038.
79. Vaze MB, Pellicioli A, Lee SE, Ira G, Liberi G, et al. (2002) Recovery from checkpoint-mediated arrest after repair of a double-strand break requires Srs2 helicase. Mol Cell 10: 373–385.
80. Wach A, Brachat A, Pohlmann R, Philippsen P (1994) New heterologous modules for classical or PCR-based gene disruptions in Saccharomyces cerevisiae. Yeast 10: 1793–1808.
81. Spencer F, Hugerat Y, Simchen G, Hurko O, Connelly C, et al. (1994) Yeast kar1 mutants provide an effective method for YAC transfer to new hosts. Genomics 22: 118–126.
82. Schober-Ditmore W, Bachant J (2000) Yeast DNA flow cytometry. In: Diamond R, DeMaggio S, eds. In Living Color: Protocols in Flow Cytometry and Cell Sorting. New York: Springer Lab Manuals. pp 455–460.
83. Warsi TH, Navarro MS, Bachant J (2008) DNA topoisomerase II is a determinant of the tensile properties of yeast centromeric chromatin and the tension checkpoint. Mol Biol Cell 19: 4421–4433.

84. Christianson TW, Sikorski RS, Dante M, Shero JH, Hieter P (1992) Multifunctional yeast high-copy-number shuttle vectors. Gene 110: 119–122.
85. Mankouri HW, Craig TJ, Morgan A (2002) SGS1 is a multicopy suppressor of srs2: functional overlap between DNA helicases. Nucleic Acids Res 30: 1103–1113.
86. Desany BA, Alcasabas AA, Bachant JB, Elledge SJ (1998) Recovery from DNA replicational stress is the essential function of the S-phase checkpoint pathway. Genes Dev 12: 2956–2970.